ФИЗИКА ЭЛЕМЕНТАРНЫХ ЧАСТИЦ И АТОМНОГО ЯДРА
2005. Т. 36. ВЫП. 5

УДК 539.12.1

CURRENT EXPERIMENTS USING POLARIZED BEAMS OF THE JINR VBLHE ACCELERATOR COMPLEX

F. Lehar

DAPNIA, CEA/Saclay, Gif-sur-Yvette Cedex, France

ФИЗИКА ЭЛЕМЕНТАРНЫХ ЧАСТИЦ И АТОМНОГО ЯДРА
2005. Т. 36. ВЫП. 5

УДК 539.12.1

CURRENT EXPERIMENTS USING POLARIZED BEAMS OF THE JINR VBLHE ACCELERATOR COMPLEX

F. Lehar

DAPNIA, CEA/Saclay, Gif-sur-Yvette Cedex, France

The present review is devoted to the spin-dependent experiments prepared at the JINR Veksler–Baldin Laboratory of High Energies and carried out at the Synchrophasotron or Nuclotron accelerators. The acceleration of polarized deuterons, experiments using the internal targets, the beam extraction and the polarimetry are briefly described. Then, representative experiments using either the extracted deuteron beam or secondary beams of polarized nucleons produced by polarized deuterons, are considered. Three current experiments: DELTA–SIGMA, DELTA, pp SINGLET, and recently BES, require the polarized nucleon beams in conjunction with the Dubna polarized proton target. Already available $\Delta\sigma_L(np)$ results from the first experiment show an unexpected energy dependence. The experiment DELTA should investigate the nucleon strangeness. The aim of the pp SINGLET is to study a possible resonant behavior of the spin-singlet pp-scattering amplitude. BES proposes the measurement of the complete experiment in dp backward elastic scattering. For all other Dubna experiments, unpolarized nucleon or nuclei targets are used. The polarized deuteron beam allows one to determine spin-dependent observables necessary for understanding the deuteron structure, as well as the nucleon substructure. One part of investigations concerns deuteron break-up reactions and deuteron–proton backward elastic scattering. A considerable amount of data was obtained in this domain. Another part is dedicated to the measurements of the same spin-dependent observables in a «cumulative» region. Interesting results were obtained for proton or pion productions in inclusive and semi-inclusive measurements. In the field of inelastic deuteron reactions, the analyzing-power measurements were performed in the region covering Roper resonances. Many existing models are in disagreement with observed momentum dependences of different results. Finally, the proton–carbon analyzing-power measurements extended the momentum region of rescattering observables. Some inclusive Dubna results are compared to exclusive Saclay data and to lepton–deuteron measurements. Finally, the pC and $p\mathrm{CH}_2$ analyzing-power data extended the momentum region of rescattering observables. Most of the JINR LHE experiments are carried out in the framework of a large international collaboration.

Настоящий обзор посвящен экспериментам с поляризованными пучками, которые были подготовлены в ЛВЭ ОИЯИ и выполнены на синхрофазотроне и нуклотроне. Коротко описаны ускорение поляризованных дейтронов, эксперименты на внутренних мишенях, вывод пучка и поляриметрия. Также описаны основные эксперименты на выведенных пучках дейтронов и на вторичных пучках поляризованных нуклонов. В трех текущих экспериментах — «Дельта–Сигма», «Дельта» и «pp-Singlet» — используются поляризованные нуклонные пучки вместе с дубненской поляризованной протонной мишенью. Результаты, полученные уже в первом эксперименте по измерению $\Delta\sigma_L(np)$, показали неожиданную зависимость данных от энергии. Эксперимент «Дельта» направлен на изучение странности нуклона. Целью третьего эксперимента является проверка возможного резонансного поведения спин-синглетной амплитуды pp-рассеяния. Все другие дубненские эксперименты используют неполяризованные мишени нуклонов или ядер. Поляризованный дейтронный пучок позволил определить зависимые от спина

величины, необходимые для изучения структуры дейтрона и нуклонной субструктуры. В одних экспериментах измеряются две зависимые от спина величины: в реакциях с развалом дейтрона и в дейтрон-протонном упругом рассеянии назад. Большое количество данных было получено в этой области. В других экспериментах измеряются те же самые наблюдаемые в кумулятивной области. Интересные результаты получены для рождения протонов и пионов в инклюзивных измерениях. Анализирующая способность измерялась в неупругих (d, d)-реакциях в области роперовских резонансов. Некоторые инклюзивные дубненские данные можно сравнить с эксклюзивными данными, полученными в Сакле, и с результатами лептон-дейтронного рассеяния. Многие существующие модели не описывают измеренные энергетические зависимости наблюдаемых величин. В заключение приведены результаты измерений анализирующей способности при рассеянии протонов на углероде, которые сдвинули границу существующих данных в сторону высоких импульсов налетающих протонов. Эти данные необходимы для измерений поляризации частиц в двойном рассеянии. Большинство экспериментов в ЛВЭ ОИЯИ выполнено в рамках широкого международного сотрудничества.

This review is dedicated to the memory of Academician Alexander Mikhailovich Baldin, who often declared that Spin Physics is even more important than the Nuclotron

INTRODUCTION

The represetative spin-dependent experiments performed or accepted at the JINR Veksler–Baldin Laboratory of High Energies (VBLHE) Synchrophasotron–Nuclotron Accelerator Complex are reviewed. Vector and/or tensor polarized deuteron beams, with vertical quantization axis, are often directly used. This axis remains practically fixed, since the deuteron magnetic momentum is small. Break-up of vector polarized deuterons produces vertically polarized neutrons and protons. Due to a large anomalous momentum of nucleons, its polarization direction along any base space vector may be obtained by rotation or precession of nucleon spins in magnetic fields.

I recall that the responsible person for the Spin Physics Programme in VBLHE (Programme No. 0941) was Academician A. M. Baldin up to April 2001. At present, the responsible persons for the scientific programme «Search for Non-Nucleon Degrees of Freedom and Spin Effects in Few-Nucleon Systems» are N. M. Piskunov, V. V. Glagolev and G. Martinská.

A major part of the experiments was carried out at the Synchrophasotron, at laboratory momenta below 5 GeV/c per nucleon. This accelerator was not in use since 2003. All machine experts concentrated on the improvement of the superconducting accelerator Nuclotron. Leaders of the development are A. D. Kovalenko and A. I. Malakhov. The planned maximal energy of 6 GeV/c per nucleon has not been achieved so far. Since the Nuclotron is an accelerator with one-turn injection, it is necessary to increase the intensity of the polarized ion source. On the other hand, slow beam extraction of 10 s was recently obtained and is practically independent of the beam intensity. A momentum spread

was determined, using the slowly extracted ^{7}Li beam [1]. The polarized deuteron beam was accelerated and its polarization was determined [2].

VBLHE experiments mainly use unpolarized LH_2, CH_2 or nuclei targets in conjunction with the extracted polarized beams. Several important JINR results were obtained using internal targets. In some investigations the extracted polarized beam and the polarized proton target (PPT) are needed. The polarized deuteron target (PDT) in Dubna could be used in the near future. It is also possible to construct internal polarized targets. In addition to a polarized jet or a cell target a polarizable thin foil, even scintillating, was developed at PSI, in collaboration with Dubna experts. This kind of target was never used in an experiment, but may be interesting for particle physics, as well as for heavy-ion accelerators.

It was impossible to treat off all VBLHE results and to give a full list of references. Most of the figures in the present review are reproduced from original publications, since numerical tables and fits are often inaccessible. Eventual mistakes in some figures are the responsibility of the authors and will be pointed out if recognized.

1. POLARIZED BEAM AND POLARIMETRY

Vector and tensor polarized deuterons from the ion source POLARIS [3] are accelerated in the linear accelerator, reach 10 MeV, and then are injected into the main ring. The responsible person for this experiment is Yu. K. Pilipenko, who was a leader of the polarized source construction.

To measure the vector and tensor deuteron beam polarizations before injection, semiconductor detector systems were installed behind the linac [4]. To determine the vector polarization [5], deuterons hit a gaseous ^{4}He target, and the left-right asymmetry in the reaction $d + {}^4\mathrm{He} \to d + {}^4\mathrm{He}$ was measured ($\theta_{\mathrm{lab}}(d) = 126^\circ$, $\theta_{\mathrm{lab}}(^4\mathrm{He}) = 15^\circ$). In the stripping reaction $d + {}^3\mathrm{He} \to p + {}^4\mathrm{He}$ [6] the tensor polarization can be determined. In this case protons were detected at $\theta = 0^\circ$. Such reactions have large vector [7] and tensor [8] analyzing powers, accurately measured. The tensor polarimeter is insensitive to the rotation of the spin quantization axis around the beam direction. This polarimeter was dismounted due to a low counting rate during the beam polarization measurements. It may be needed again for the Nuclotron ion source tuning.

A recoil-particle spectrometer installed inside the Synchrophasotron ring [9] also existed. It was used to determine the vector polarization from the measured left-right proton asymmetry in the elastic dp scattering. A thin polyethylene target foil of several μm was inserted in the internal beam when a desired deuteron energy was achieved. Multiple particle passage through this target insured good statistical accuracy because of a rather large luminosity. Recoil protons, ejected at $\theta_{\mathrm{lab}} = 82.5^\circ$ were identified in two semiconductor detector telescopes.

Several experiments were performed at this polarimeter, e.g., Ref. 10. In this measurement the vector analyzing power for the elastic dp and dd scattering in the momentum interval from 2.38 to 10 GeV/c and for the inelastic reaction $d + \mathrm{C} \to p + X$ at 2.38 GeV/c were determined. For elastic processes the $-t$ interval was from 0.005 to 0.054 (GeV/c)^2. In the inelastic interactions, protons in the energy interval 40–300 MeV were recorded at the laboratory angles of 75 and 120°. Figure 1 shows A_y at $-t = 0.025$ (GeV/c)^2 as a function of deuteron momentum per nucleon. The momentum dependence can be described in the generalized Glauber–Sitnenko model by the approximate formula [11].

$$A_y^{dp}(t,s) = 1/3(A_{00n0}^{pp}(t,s) + A_{00n0}^{np}(t,s)). \tag{1}$$

Equation (1) is satisfied within the errors and gives an indirect confirmation of the deuteron polarization P_d preservation during the acceleration (see below).

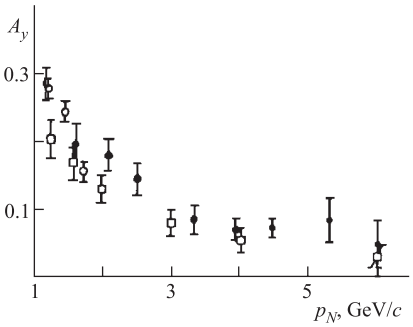

Fig. 1. Vector analyzing power A_y of elastic $d \uparrow p$ scattering as a function of momentum (per nucleon) of the beam: ● — [10], ○ — calculation using Eq. (1) [11]. See comment in the text

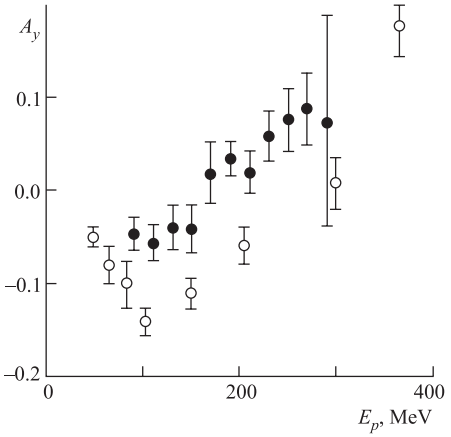

Fig. 2. Vector analyzing power A_y as a function of the kinetic energy of the detected protons at the laboratory angle of 75° for $d \uparrow \mathrm{C} \to pX$ (● — [10]) and $p \uparrow \mathrm{C} \to pX$ (○ — [12])

Some JINR physicists claim a mistake in Fig. 1, concerning the plotted point at 6 GeV/c per nucleon. The reason is that the deuteron momentum of 12 GeV/c cannot be reached at the Synchrophasotron. On the other hand, the authors of [4] (see below) clearly have stated that the primary deuteron beam up to 12 GeV/c in Ref. 10 has been used.

Figure 2 shows A_y for $d + \mathrm{C} \to p + X$ at 2.38 GeV/c and at 75° as a function of the detected proton energy. The Dubna data [10] are compared with

the analyzing power data from $p+\mathrm{C} \to p+X$ at 1.49 GeV/c [12]. No quantitative models for an explanation of the difference exist. A qualitative conclusion can be drawn that at low energy of secondary protons the role of rescattering of nucleons in the $d + \mathrm{C}$ reaction is important.

The internal polarimeter at the Synchrophasotron has been dismounted, but it was obvious that an internal target station will be needed for the Nuclotron. Such a station was studied [13–15]. The first experiment at the Nuclotron was performed using internal targets [16]. Unpolarized deuterons were accelerated up to 200 MeV, very thin polyethylene, copper and gold foils were inserted and products of interaction were measured.

Acceleration of polarized deuterons required a polarimeter with the internal hydrogenous target [17]. Recently, such a polarimeter was constructed as described by JINR (Dubna) and SAS (Bratislava) groups [2]. It consists of two forward arms F_L, F_R, each of them equipped by three scintillation counters and two backward arms B_L, B_R, each equipped by two counters. The pairs F_L, B_R and F_R, B_L are positioned at conjugate angles of pp kinematics, depending on the energy. Measurements give left-right asymmetries at the proton momentum p_p equal to one half of deuteron momentum p_d.

The vector polarized deuteron beam was scattered on the CH_2 and carbon targets. A thin polyethylene foil (10 μm) or ten carbon wires of 8 μm in diameter, respectively, were fixed on the frame, which was inserted into the beam at the desired energy. The asymmetry of quasi-elastic $(pn) + p \to p + p$ scattering was measured, considering the deuteron as a weakly bound proton and neutron. The equality of spin-dependent observables for elastic and quasi-elastic pp, np, and pn scattering on light nuclei has been studied over a large energy region (e.g., [18, 19]) and holds in the Dubna conditions.

The results in [2] were carried out at the deuteron beam momenta of 3.0, 3.5, 3.8, and 5.0 GeV/c (i.e., 0.83, 1.05, 1.18, and 1.73 GeV proton energy) and the beam polarization was deduced using the pp analyzing power data from [20]. The measured deuteron beam polarization is constant in the studied interval ($P_d^+ = -P_d^- \simeq 0.60$). The data agree with the results obtained independently at the extracted beam polarimeter [21]. In principle, the slow beam extraction could affect the internal polarimeter results, e.g., by changing the beam position in the ring, etc. The authors concluded that no dependence on the beam extraction was observed and the internal polarimeter can be used simultaneously with beam-line experiments.

Other Dubna experiments, measuring the deuteron beam polarizations, were carried out with extracted polarized deuterons. One of the first experiments of this kind is described in Ref. 22. At the fast extraction beam line, a 100 cm liquid hydrogen bubble chamber has been exposed to vector polarized deuterons. The break-up reaction $dp \to ppn$ has been studied at 3.34 GeV/c and the azimuthal asymmetry of the outgoing nucleons has been measured. The pp and np

elastic scattering analyzing powers, measured at the ANL-ZGS and at Saturne II were used in order to deduce the beam vector polarization. Its absolute value was found to be $|P_d| = 0.41 \pm 0.09$, considerably lower than actual values at the Synchrophasotron and Nuclotron. Asymmetry measurements were also reported in [23].

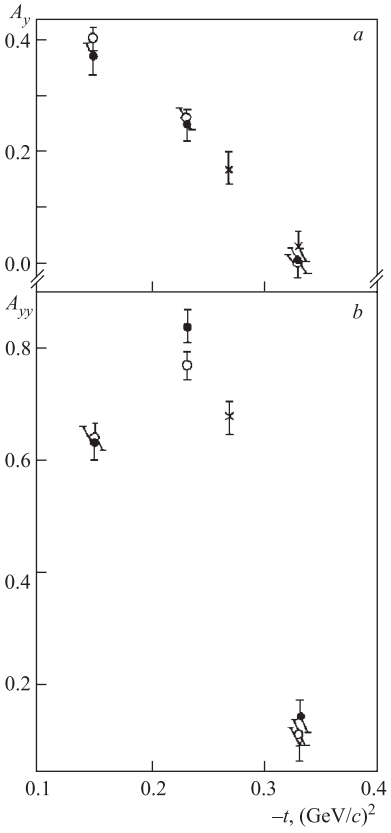

Fig. 3. Vector and tensor analyzing powers A_y (a) and A_{yy} (b) vs. four-momentum transfer. The Dubna data (crosses) are compared with the ones of Saclay [27, 28]

The slow extraction of the beam into different beam lines [24] gave the possibility to perform fast detectors. The average intensity of the Synchrophasotron polarized beams, started in 2001, turned around $3 \cdot 10^9$ deuterons/cycle. The vector polarization value is checked by two kinds of beam polarimeters. Any of them measures elastic scattering asymmetries and needs a knowledge of corresponding analyzing powers.

In the first method, the $dp \to dp$ asymmetry is measured by the four-arm polarimeter. Deuterons scattered on the liquid hydrogen target are analyzed by a magnetic field of the two-arm magnetic spectometer ALPHA [4, 25]. The deuteron kinetic energy was set at 1.6 GeV. At this energy, the vector and tensor analyzing powers in angular distributions of the dp elastic scattering are known from the Saturne II data [26]. A_y and A_{yy} are applied to the measured asymmetries. The scattering angle is fixed close to the maximal values of the vector and tensor analyzing powers, respectively. The polarimeter can work at high beam intensities. On the other hand, the measurements often require changing the deuteron energy and/or extracting deuterons in another beam line, which is a time-consuming operation. A major part of the beam polarization measurements has been carried out using this polarimeter.

With the dp polarimeter, A_y and A_{yy} at fixed angle were measured at 3.0, 4.0, and 4.5 GeV/c [4]. The $-t$ (GeV/c)^2 dependences of these quantities were obtained at Saturne II [27,28] at 3 GeV/c by varying the scattering angle. Figure 3 shows that the results obtained in different methodical procedures agree with each other.

The second method consists in the left-right asymmetry measurement of the quasi-elastic $(pn)p$ scattering, similarly as described for the internal polarimeter. The four-arm beam polarimeter with small acceptance of $7.1 \cdot 10^{-4}$ sr, using polyethylene and carbon targets, was constructed by the Gatchina and JINR groups in 1995 [29]. It was considerably improved in 1997 [21]. The asymmetries were measured at $\theta_{\rm lab} = 14^\circ$ below the deuteron beam momenta $p_d = 6$ GeV/c and at 8° at higher p_d. A calibration was carried out at the 1.6 GeV deuteron energy, where pC asymmetry was subtracted, and accurately measured LAMPF and Saturne II analyzing power data were applied. The calibration is discussed in [30]. The results agree with the data measured using the dp polarimeter. The deuteron vector beam polarization measurements at different energies were published in [20, 31]. The responsible person for the pp polarimeter operation is L. S. Azhgirey.

The pp polarimeter provides a continuous check of the beam polarization stability at any energy, during the data acquisition period. It is used in experiments with polarized nucleons. On the other hand, this polarimeter checks the deuteron vector polarization only.

The polarimeter POMME [32], which was widely used at Saclay, was transported to Dubna and installed as a part of the detection system of the ALPHA spectrometer [4, 25]. It is called ALPOM. This apparatus was not generally used for the beam polarimetry and the relevant experiments will be discussed in Sec. 6.

In order to decrease possible systematic errors, absolute calibration measurements of the deuteron vector and tensor polarizations were proposed in [33]. For the vector beam polarization the suggestion is based on the equality of the analyzing power A and the polarization of the scattered particle P in the elastic scattering (e.g., $pp \to pp$ or $dp \to dp$), assuming time-reversal invariance (TRI). The author proposes to use the pp beam polarimeter (see above) and the SPHERE [34–37] experimental setup for the A and P measurements, respectively. The tensor polarization is suggested to be determined by measurement of the tensor analyzing power T_{20}, assuming that the unpolarized dp cross section is known.

The deuteron vector polarization, or the polarization of break-up nucleons, can be determined from asymmetry measurements using a polarized beam and/or target. For this purpose the beam and target polarizations $\mathbf{P}_B^+ = -\mathbf{P}_B^-$ and $\mathbf{P}_T^+ \neq -\mathbf{P}_T^-$ are oriented along the normal to the scattering plane ($\mathbf{n}$). The most general formula for the correlated nucleon–nucleon (NN) scattering cross section from Ref. 38 is considerably simplified. We have

$$d\sigma/d\Omega = (d\sigma/d\Omega)_0 \, (1 + A_{00n0} P_{Bn} + A_{000n} P_{Tn} + A_{00nn} P_{Bn} P_{Tn}) \qquad (2)$$

for four combinations of $\pm P_{Bn}$ and $\pm P_{Tn}$. Here $(d\sigma/d\Omega)_0$ is the differential cross section for single scattering of unpolarized incident and target particles. It

depends, as well as all observables, on the single-scattering angle $\theta_{\rm cm}$. A_{00n0} and A_{000n} are the beam and target analyzing powers, respectively, and A_{00nn} is the spin-correlation coefficient. Following the NN formalism and notations [38], the subscripts of any observable $X_{\rm srbt}$ refer to the polarization states of the scattered, recoil, beam, and target particles, in this order. In our case $s = r = 0 = \circ$, $b = n, \circ$, $t = \circ, n$.

Four asymetries measured with polarized beam and target, determine the three products in brackets of Eq. (2). Two other asymmetries can be measured using either polarized beam and unpolarized target, or vice versa. These measurements determine $A_{00n0}P_{Bn}$ or $A_{000n}P_{Tn}$ in Eq. (2), respectively. From Pauli principle, applied to pp elastic scattering, it holds $A_{00n0} = A_{000n}$. If $\pm P_{Tn}$ are accurately known, A_{000n} can be deduced and used to determine P_{Bn}. It is obvious that this method is independent of the beam energy. The method could be used, when the PPT polarization, perpendicular to the beam direction will be available (see the next section). It needs a construction of a dedicated polarimeter at PPT.

Problems with acceleration of polarized protons or deuterons in any ring-type accelerator are mainly related to depolarizing resonances. Theory of these effects was written by Froisard and Stora [39], first calculations concerning the acceleration of polarized deuterons were carried out by Plis and Soroko [40] (see review [41] and references therein for details).

There are basically two types of depolarizing resonances: the first is the so-called «closed-orbit resonance», often referred to as an «imperfection resonance» (Type I), which affects all beam particles equally; the second (Type II) resonance depends on the position of each beam particle during the acceleration. Type-II resonances are due to the focusing elements in the ring and to the nonzero emittance of the accelerated particles. They are characterized by

$$\gamma G = \pm k, \tag{3}$$

$$\gamma G = \pm \ell \pm m\nu_x \pm n\nu_z \tag{4}$$

for Type I and Type II, respectively, where G is the gyromagnetic anomaly ($G_p = 1.792847$ and $G_d = -0.14256$ in nuclear magneton units); ℓ, k, q, m, n are positive integers; ν_x, ν_z are the betatron horizontal and vertical wave numbers, and γ is the relativistic energy factor.

Taking the masses $M_p = 0.9382723$ GeV and $M_d = 1.875869$ GeV, the lowest lying Type-I deuteron depolarizing resonance occurs for $k = -1$ at $T_{\rm kin}(d) = 11.28$ GeV (momentum $p_{\rm lab}(d) = 13.02$ GeV/c). For protons this effect already occurs at 108.4 MeV, where $k = +2$. Due to this fact, polarized protons cannot be simply accelerated at the Synchrophasotron–Nuclotron complex without considerable changes of the accelerator rings. On the other hand, the deuteron beam energy of each Dubna accelerator is always lower than the lowest lying Type-I depolarizing resonance.

Due to Type-II resonances and other possible instrumental sources the beam depolarization may exist. It can be determined by the so-called «deceleration method» which consists in two asymmetry measurements with the same polarimeter setting and at the same low energy T_1. The first measurement is carried out, when the deuteron beam is extracted, reaching T_1. Then the beam is accelerated up to some high energy T_2 without extraction, then decelerated down to the energy T_1 and extracted. The difference of the two measured asymmetries reveals a possible beam depolarization.

The deceleration method was developed at Saturne II [42] for accelerated polarized protons, but it was too expensive to construct a slow extraction for the decelerated beam. During the deceleration, protons were extracted within few μs only and the measurements were time-consuming. Moreover, the experiment with protons must be repeated for any maximal energy used, since many depolarizing resonances occur.

The Synchrophasotron experts in VBLHE constructed the slow extraction during the deceleration very succesfully and rapidly. Measurements of the deuteron vector analyzing power were carried out using the dp polarimeter [4], described above. The deuteron beam was first extracted when reaching the momentum $p_{\mathrm{lab}}(d) = 3$ GeV/c. Then the beam was accelerated up to 9 GeV/c, then decelerated down to 3 GeV/c and extracted. The measured ratio of the vector polarization values, obtained with these two beams, turned out to be constant within 4%. The authors concluded that no appreciable depolarizing effects exist up to 9 GeV/c [4]. Consequently, the deuteron beam vector and tensor polarizations at the Synchrophasotron are independent of energy, and it is sufficient to determine them at one energy only. It will be necessary to provide the same test at the Nuclotron.

The deceleration method is to be considered as a polarimetry tool. It is also relative, but it considerably reduces a systematic error. Today, this method is used, e.g., at COSY for polarized protons.

2. EXPERIMENTS WITH POLARIZED NUCLEONS AND PPT

In this section the three current experiments using polarized nucleon beam and the polarized proton target (PPT) are treated. A large Argonne–Saclay PPT, 20 cm long and 3 cm in diameter, was transported to Dubna and reconstructed in the Dzhelepov Laboratory of Nuclear Problems (DLNP) during 1994 by Russian, Ukrainian, and French experts as a «movable polarized target» (MPT) [43–45]. It was installed at the Synchrophasotron beam line and used in the first experiment in March 1995. During 1996 and 1997 a new polarizing solenoid for the PPT was constructed in VBLHE [46]. Only the target polarization in the longitudinal direction could be obtained at the moment. The MPT is to be completed by

the vertical superconducting holding coils, constructed in Kharkov and tested recently in Dubna. The target can work using hydrogenous as well as deuterated polarizable compounds, including ^{6}LiD (MDT). It is operated by the international «polarized target group» from several laboratories, under the responsibility of Yu. A. Usov. Spokespersons for the target development are E. A. Matyushevsky and N. S. Borisov.

The MPT can be considered as one of the «basic facilites» at JINR. It can be pointed out that a part of VBLHE experiments, listed in Secs. 3, 4, and 5, using unpolarized proton or deuteron targets, could be carried out with the MPT or MDT. In this case, existing results will appear as by-products of measurements, using both polarized deuteron beam in conjunction with the polarized target. This possibility was widely discussed by physicists working in different fields of VBLHE activities. The relevant measurements of the d, p and $^3\mathrm{He}, d$ backward elastic scattering (BES) were recently proposed. The JINR Program Advisory Committee (PAC) for Particle Physics supported this new program and recommended it in 2003. The BES experiment is discussed in Subsec. 3.2.

2.1. DELTA–SIGMA Experiment. The aim of the JINR experimental programme «DELTA–SIGMA Experiment» is to obtain data sets of np observables over the Dubna neutron energy region, sufficient to perform a direct reconstruction of the scattering amplitudes (DRSA) in the forward direction. The imaginary parts can be determined unambigously from measurements of three total np cross sections. The determination of real parts require a knowledge of three additional independent np quantities (at least). Isosinglet ($I = 0$) amplitudes at $\theta = 0$ can be deduced from the np data, assuming that the isotriplet ($I = 1$) system is known. The responsible person for this experimental programme is V. I. Sharov, the spokespersons are L. N. Strunov and V. I. Sharov.

The general expression of the total cross section for a polarized nucleon beam transmitted through a PPT, with arbitrary directions of beam and target polarizations, $\mathbf{P}_B$ and $\mathbf{P}_T$, respectively, was first deduced by Bilenky and Ryndin [47] and independently by Phillips [48] in 1963. Assuming parity conservation, TRI and isospin invariance (or Pauli principle for identical particles), the total cross section is written in the form:

$$\sigma_{\mathrm{tot}} = \sigma_{0\mathrm{tot}} + \sigma_{1\mathrm{tot}}(\mathbf{P}_B, \mathbf{P}_T) + \sigma_{2\mathrm{tot}}(\mathbf{P}_B, \mathbf{k})(\mathbf{P}_T, \mathbf{k}), \tag{5}$$

where $\mathbf{k}$ is a unit vector in the direction of the beam momentum. The term $\sigma_{0\mathrm{tot}}$ is the total cross section for unpolarized particles, $\sigma_{1\mathrm{tot}}$, $\sigma_{2\mathrm{tot}}$ are the spin-dependent contributions. They are related to the measurable observables $\Delta\sigma_T$ and $\Delta\sigma_L$ by:

$$-\Delta\sigma_T = 2\sigma_{1\mathrm{tot}}, \tag{6}$$

$$-\Delta\sigma_L = 2(\sigma_{1\mathrm{tot}} + \sigma_{2\mathrm{tot}}), \tag{7}$$

called «total cross-section differences». The negative signs for $\Delta\sigma_T$ and $\Delta\sigma_L$ in Eqs. (6) and (7) correspond to the usual, although unjustified, convention in the literature. The total cross-section differences are measured with either parallel or antiparallel beam and target polarization directions. Polarization vectors are transversally oriented with respect to the beam direction for $\Delta\sigma_T$ measurements and longitudinally oriented for $\Delta\sigma_L$ experiments [38, 41].

For $\mathbf{P}_B^{\pm}$ and $\mathbf{P}_T^{\pm}$, all oriented along $\mathbf{k}$, one obtains four total cross sections:

$$\sigma(\rightrightarrows) = \sigma(++) = \sigma_{0\mathrm{tot}} + |P_B^+ P_T^+|\ (\sigma_{1\mathrm{tot}} + \sigma_{2\mathrm{tot}}), \tag{8a}$$

$$\sigma(\leftrightarrows) = \sigma(-+) = \sigma_{0\mathrm{tot}} - |P_B^- P_T^+|\ (\sigma_{1\mathrm{tot}} + \sigma_{2\mathrm{tot}}), \tag{8b}$$

$$\sigma(\rightleftarrows) = \sigma(+-) = \sigma_{0\mathrm{tot}} - |P_B^+ P_T^-|\ (\sigma_{1\mathrm{tot}} + \sigma_{2\mathrm{tot}}), \tag{8c}$$

$$\sigma(\leftleftarrows) = \sigma(--) = \sigma_{0\mathrm{tot}} + |P_B^- P_T^-|\ (\sigma_{1\mathrm{tot}} + \sigma_{2\mathrm{tot}}). \tag{8d}$$

The arrows and signs in brackets correspond to the $\mathbf{P}_B$ and $\mathbf{P}_T$ directions with respect to $\mathbf{k}$. An arbitrary pair of one parallel and one antiparallel beams and target polarization directions determines $\Delta\sigma_L$. By using two independent pairs, an instrumental asymmetry term (IA) is removed. The formulae for the transversal polarizations are similar.

Since the $\mathbf{P}_B$ direction could be reversed at every cycle of the accelerator, it is preferable to calculate $\Delta\sigma_L$ from the pairs $(\rightrightarrows)$, $(\leftrightarrows)$, and $(\rightleftarrows)$, $(\leftleftarrows)$, measured with the same $\mathbf{P}_T$ orientation. This eliminates long-time efficiency fluctuations of the detectors. The spin-averaged term $\sigma_{0\mathrm{tot}}$ drops out when taking the differences, and one obtains:

$$-\Delta\sigma_L(P_T^+) = 2\ (\sigma_{1\mathrm{tot}} + \sigma_{2\mathrm{tot}})^+ = \frac{2\ [\sigma(\rightrightarrows) - \sigma(\leftrightarrows)]}{(|P_B^+| + |P_B^-|)\ |P_T^+|}, \tag{9a}$$

$$-\Delta\sigma_L(P_T^-) = 2\ (\sigma_{1\mathrm{tot}} + \sigma_{2\mathrm{tot}})^- = \frac{2\ [\sigma(\leftleftarrows) - \sigma(\rightleftarrows)]}{(|P_B^+| + |P_B^-|)\ |P_T^-|}. \tag{9b}$$

Each of relations (9a) and (9b) contains a hidden contribution from the instrumental asymmetry IA:

$$\mathrm{IA} = [\Delta\sigma_L(P_T^+) - \Delta\sigma_L(P_T^-)]/2. \tag{10}$$

IA cancels out, giving the final results as a simple average

$$\Delta\sigma_L = [\Delta\sigma_L(P_T^+) + \Delta\sigma_L(P_T^-)]/2\ . \tag{11}$$

The scattering matrix can be written in the form [38]

$$M(\mathbf{k}_f, \mathbf{k}_i) = \frac{1}{2}[(a+b) + (a-b)(\boldsymbol{\sigma}_1, \mathbf{n})(\boldsymbol{\sigma}_2, \mathbf{n}) + (c+d)(\boldsymbol{\sigma}_1, \mathbf{m})(\boldsymbol{\sigma}_2, \mathbf{m}) + \\ + (c-d)(\boldsymbol{\sigma}_1, \mathbf{l})(\boldsymbol{\sigma}_2, \mathbf{l}) + e(\boldsymbol{\sigma}_1 + \boldsymbol{\sigma}_2, \mathbf{n})], \tag{12}$$

where a, b, c, d, and e are five complex scattering amplitudes, which are functions of energy and scattering angle $\theta_{\rm CM}$; $\boldsymbol{\sigma}_1$ and $\boldsymbol{\sigma}_2$ are the Pauli 2×2 matrices; $\mathbf{k}_i$ and $\mathbf{k}_f$ are the unit vectors in the direction of the incident and scattered particles, respectively, and

$$\begin{gathered}\mathbf{n}=(\mathbf{k}_i\times\mathbf{k}_f)/|\mathbf{k}_i\times\mathbf{k}_f|,\ \mathbf{l}=(\mathbf{k}_f+\mathbf{k}_i)/|\mathbf{k}_f+\mathbf{k}_i|,\\ \mathbf{m}=(\mathbf{k}_f-\mathbf{k}_i)/|\mathbf{k}_f-\mathbf{k}_i|.\end{gathered}\tag{13}$$

The scattering matrix simplifies at forward $\theta=0$ and backward $\theta=\pi$ angles. The amplitudes in (13) then satisfy

$$a(0)-b(0)=c(0)+d(0),\quad e(0)=0,\tag{14a}$$

$$a(\pi)-b(\pi)=c(\pi)-d(\pi),\quad e(\pi)=0.\tag{14b}$$

The quantities $\sigma_{0\rm tot}$, $\Delta\sigma_T$, and $\Delta\sigma_L$ for pp and np transmission are linearly related to the imaginary parts of the three independent forward scattering amplitudes $a+b$, c and d [38] via optical theorems:

$$\sigma_{0\rm tot}=(2\pi/K)\ \mathrm{Im}\, m\ [a(0)+b(0)],\tag{15}$$

$$-\Delta\sigma_T=(4\pi/K)\ \mathrm{Im}\, m\ [c(0)+d(0)],\tag{16}$$

$$-\Delta\sigma_L=(4\pi/K)\ \mathrm{Im}\, m\ [c(0)-d(0)],\tag{17}$$

where K is the wave number. Note that the optical theorems always provide the absolute amplitudes, as discussed in [49–51]. From Eqs. (14) to (17) the partial DRSA unambiguously determines the imaginary parts of the nonvanishing amplitudes.

The scattering matrices for pp, np, and nn are given in terms of isosinglet (M_0) and isotriplet (M_1) matrices, both in the form of Eq. (12).

$$M(\mathbf{k}_f,\mathbf{k}_i)=\frac{M_0}{4}[1-(\boldsymbol{\tau}_1,\boldsymbol{\tau}_2)]+\frac{M_1}{4}[3+(\boldsymbol{\tau}_1,\boldsymbol{\tau}_2)],\tag{18}$$

where $\boldsymbol{\tau}_1$ and $\boldsymbol{\tau}_2$ are the nucleon isospin matrices. We have

$$M(pp\to pp)=M(nn\to nn)=M_1,\tag{19a}$$

$$M(np\to np)=M(pn\to pn)=(M_1+M_0)/2.\tag{19b}$$

From Eqs. (19a), (19b) one obtains any $np\to np$ amplitude Ampl, at $\theta_{\rm cm}$:

$$\mathrm{Ampl}(np)=\left(\mathrm{Ampl}(I=1)+\mathrm{Ampl}(I=0)\right)/2.\tag{20}$$

Applying Eq. (20) to the measured $\Delta\sigma(np)$ values and the existing $\Delta\sigma(pp)$ data at the same energy, from Eqs. (15) and (16) one deduces

$$\sigma_{0\mathrm{tot}}(I=0) = 2\sigma_{0\mathrm{tot}}(np) - \sigma_{0\mathrm{tot}}(pp), \tag{21a}$$

$$\Delta\sigma_{L,T}(I=0) = 2\Delta\sigma_{L,T}(np) - \Delta\sigma_{L,T}(pp). \tag{21b}$$

The total cross-section differences $\Delta\sigma_{L,T}$ for pp scattering were first measured at the ANL-ZGS and then at TRIUMF, in PSI, at LAMPF, Saturne II and in Fermilab. Results were obtained in the energy range from 0.2 to 12 GeV and at 200 GeV. Measurements with incident charged particles need an experimental setup different from neutron–proton experiments, due to the contribution of electromagnetic interactions. Existing $\Delta\sigma_{L,T}(pp)$ results were discussed in the review [41] and references therein.

$\Delta\sigma_L(pn)$ results from 0.51 to 5.1 GeV were deduced for the first time in 1981 from the $\Delta\sigma_L(pd)$ and $\Delta\sigma_L(pp)$ measurements at the ANL-ZGS [52]. These pn results were omitted in many existing databases, due to uncertainties in the Glauber-type rescattering corrections (see [41]).

$\Delta\sigma_T(np)$ and $\Delta\sigma_L(np)$ results were obtained at 11 and 10 energies, respectively, in the energy range from 0.31 to 1.10 GeV, using free polarized neutrons at Saturne II [53–55]. The Saclay results were soon followed by PSI measurements [56] at 7 energy bins from 0.180 to 0.537 GeV, using a continuous neutron energy spectrum. The PSI and Saclay sets allowed one to deduce imaginary parts of np and $I = 0$ spin-dependent forward scattering amplitudes [41, 55]. Only $\Delta\sigma_L(np)$ has been measured at five energies between 0.484 and 0.788 GeV at LAMPF [57]. There, a quasi-monoenergetic polarized neutron beam was produced in $pd \to n + X$ scattering of longitudinally polarized protons.

To be complete, at low energies, $\Delta\sigma_L(np)$ was measured at 66 MeV at the PSI injector [58], and at 16.2 MeV in Charles University, Prague [59]. $\Delta\sigma_T(np)$ was determined in Triangle Universities Nuclear Laboratory (TUNL, Durham NC) at 9 energies between 3.65 and 11.6 MeV [60], and at 16.2 MeV in Prague [61]. Finally, in TUNL $\Delta\sigma_L(np)$ was measured at 6 energies between 4.98 and 19.7 MeV [62] and $\Delta\sigma_T(np)$ at 3 other energies between 10.7 and 17.1 MeV [63]. PPT in Prague has been constructed in a narrow collaboration with Dubna experts and all measurements were carried out together with JINR physicists.

The measurements of the total cross-section differences over the Dubna Synchrophasotron neutron beam energy range have been proposed in the early 1990 [64,65]. At the beginning of 1995, the first three $\Delta\sigma_L(np)$ data points were successfully measured at the central energies 1.19, 2.49, and 3.65 GeV [66,67]. They were completed in 1997 by measurements at 1.59, 1.79, and 2.20 GeV [68, 69]. In 2001 four other points were obtained at 1.39, 1.69, 1.89, and 1.99 GeV and were published in Ref. 70.

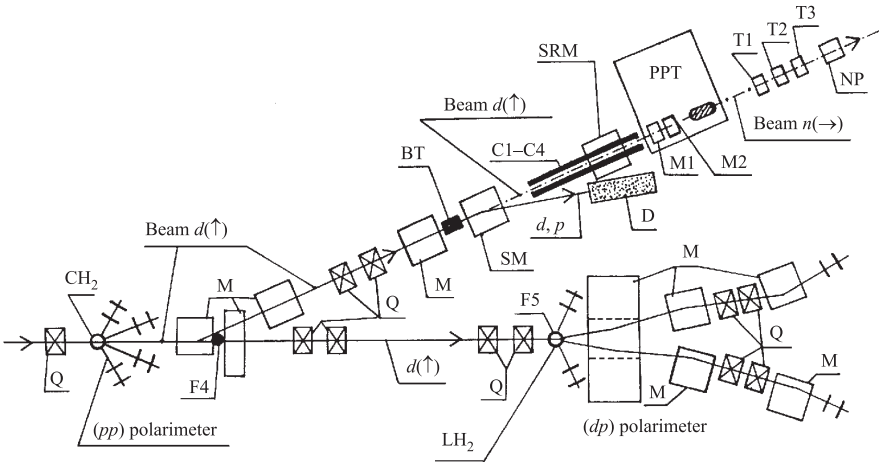

Fig. 4. Layout of the beam lines in the experimental hall (not in the scale). Full lines — vector polarized deuteron beams with $\mathbf{P}_B(d)$ oriented along the vertical direction $d(\uparrow)$; dashed line — polarized neutron beam; $n(\uparrow)$ — neutrons polarized vertically; $n(\rightarrow)$ — neutrons polarized longitudinally; BT — neutron production target; D — beam-dump for charged particles; SM — sweeping magnet; SRM — spin rotating magnet; M — dipole magnets; Q — quadrupoles; C1 to C4 — neutron beam collimators; M1, M2, T1–T3 — neutron detectors; PPT — polarized proton target; NP — neutron beam profile monitor; LH_2 — liquid hydrogen target of the *dp* polarimeter; CH_2 — target of the *pp* polarimeter; F4, F5 — focal points

The free polarized neutron beam was produced by break-up of vector polarized deuterons extracted from the Synchrophasotron. This accelerator provides the highest energy (3.7 GeV) polarized neutron beam, that can be reached at the present moment. The $\mathbf{P}_B$ direction could be reversed every cycle.

The $\Delta\sigma_L(np)$ experimental setup was described in [66–69]. Figure 4 shows both polarized deuteron and polarized free neutron beam lines [71], the two polarimeters [4,21], the beryllium target (BT) for neutron production, the collimators C1–C4, the spin rotation magnet (SRM), PPT [44–46], the neutron beam intensity monitors M1, M2, the transmission detectors T1, T2, T3 and the neutron beam profile monitor NP. The associated electronics was described in [66,67]. The system of data acquisition is based on CAMAC parallel branch highway controlled by IBM PC, using the branch driver [72]. The on-line program in «Pascal» works under DOS.

The values and directions of the neutron and proton polarizations after break-up, $\mathbf{P}_B(n)$ and $\mathbf{P}_B(p)$, respectively, are the same as the vector polarization $\mathbf{P}_B(d)$ of the incident deuteron beam [73, 74]. In order to change the vertical

orientation of the neutron beam polarization to the longitudinal direction, a spin-rotating magnet (SRM) was used. During the data acquisition, the positions and $X-Y$ profiles were monitored by the neutron beam profile monitor NP, placed close downstream from the last transmission detector.

The PPT material used in [66–69] was 1,2-propanediol ($C_3H_8O_2$ and 1-pentanol ($C_5H_{12}O$ + 5% H_2O) for 2001 experiment. The PPT polarization $P_T^{\pm}$ was measured using a computer-controlled NMR system. It was reversed once per few hours.

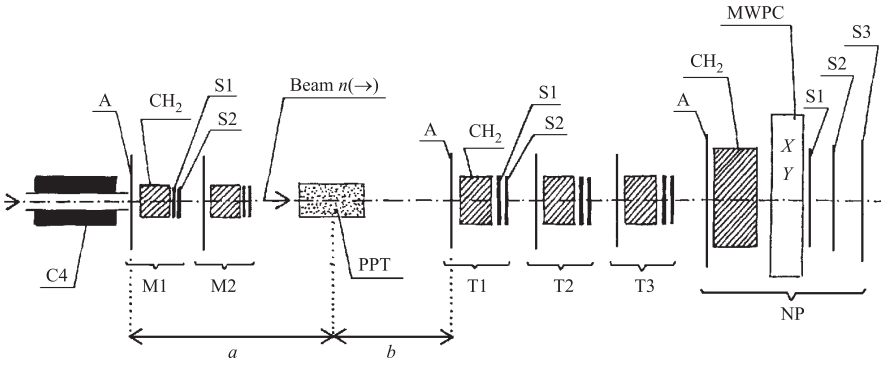

Fig. 5. Experimental setup for the $\Delta\sigma_L(np)$ measurement (not in the scale). C4 — last neutron beam collimator, 25 mm in diameter; M1, M2 — monitor neutron detectors; T1–T3 — transmission neutron detectors; NP — neutron beam profile monitor; CH_2 — converters (dimensions in the text); A — anticoincidence scintillation counters; S1–S3 — coincidence scintillation counters; MWPC — two multiwire proportional chambers, distance $a = 235$ cm, distance $b = 655$ cm

The configuration of the two neutron intensity monitors M1 and M2 and the three transmission detectors T1, T2, and T3 is shown in Fig. 5. Each of the detectors has to be independent of any other. All the units are of similar design [53] and the electronics are identical [66, 67]. Each unit consisted of a CH_2 converter, 60 mm thick, placed behind the large veto scintillation counter A. The emitted forward charged particles, generated by neutron interactions in the converter matter, were detected by two counters S1 and S2 in coincidence. Each of the neutron detector used provides a very good stability of detection efficiency. The efficiencies of $\approx 2\%$ for all detectors are practically constant with energy.

The NP array, also shown in Fig. 5, is similar to the neutron detectors. The two multiwire proportional chambers behind the converter were protected by veto A of the NP array and triggered by S1, S2, and S3 counters in coincidence.

Any transmission experiment measures the part of incident beam particles, which remain in the beam after its passage through the target. For the experiments

with incident neutrons this measurement is always relative. The neutron beam intensity is monitored by neutron beam monitors M, and outgoing particles are detected in the transmission detectors T.

With an unpolarized beam and/or target a simple transmission ratio is measured. If $N_{\rm in}$ is the number of neutrons entering the target and $N_{\rm out}$ is the number of neutrons transmitted in a counter array of solid angle Ω, then the total cross section $\sigma_{\rm tot}(\Omega) = \sigma_{0\rm tot}(\Omega)$ is related to measured quantities:

$$\frac{N_{\rm out}}{N_{\rm in}} = \exp\bigl(-\sigma_{0\rm tot}(\Omega) \times n \times d\bigr), \tag{22}$$

where n is the number of all target atoms per cm^3; d is the target length, and $N_{\rm out}/N_{\rm in}$ is the simple transmission ratio. The number of counts of the beam monitor M and of the transmission counter T depend on the efficiency η of each detector, i.e., $\mathrm{M} = N_{\rm in} \times \eta(\mathrm{M})$ and $\mathrm{T} = N_{\rm out} \times \eta(\mathrm{T})$. The extrapolation of $\sigma_{0\rm tot}(\Omega)$ towards $\Omega = 0$ gives the unpolarized total cross section $\sigma_{0\rm tot}$.

Tests of the experimental setup were performed during additional runs with high-intensity unpolarized deuteron beams, extracted either from the Synchrophasotron, or from the Nuclotron. Neutron beam energies were 1.3, 1.4, and 1.5 GeV. PPT was removed and either liquid hydrogen, or carbon targets were inserted in the neutron beam line. The measurements allowed one to determine the total cross sections $\sigma_{0\rm tot}(np)$ and $\sigma_{0\rm tot}(n\mathrm{C})$ [70].

In the $\Delta\sigma_L(\Omega)$ measurements only the number of polarizable hydrogen atoms $n_{\rm H}$ in PPT is important, because $\sigma_{\rm tot}(\Omega)$ depends on the polarizations $P_B^{\pm}$ and $P_T^{\pm}$ as shown in Eqs. (8). If one sums up the events taken with one fixed target polarizations P_T^+ or P_T^- and using Eqs. (9a) or (9b), the double transmission ratios of the measurements with the averaged $|P_B| = (|P_B^+| + |P_B^-|)/2$ for the two $\mathbf{P}_T$ directions become

$$\frac{N_{\rm out}(++)/N_{\rm in}(++)}{N_{\rm out}(-+)/N_{\rm in}(-+)} = \exp\ \left(-\Delta\sigma_L(\Omega)\ |P_B\ P_T^+| n_H d\right), \tag{23a}$$

$$\frac{N_{\rm out}(--)/N_{\rm in}(--)}{N_{\rm out}(+-)/N_{\rm in}(+-)} = \exp\ \left(-\Delta\sigma_L(\Omega)\ |P_B\ P_T^-| n_H d\right). \tag{23b}$$

The notations of Eqs. (8) are used. Thus the neutron detector efficiencies drop out. The extrapolation of $\Delta\sigma_L(\Omega)$ towards $\Omega = 0$ is to be neglected due to the small sizes of detectors [66–70]. Equations (23a), (23b) together with (10), (11) are used to determine IA and $\Delta\sigma_L$ from the measured transmission ratios.

The np data measured in Dubna are plotted in Fig. 6 as black symbols. They smoothly connect with the existing free-neutron data from [53, 54, 56, 57]. The JINR data show a fast unexpected decrease above 1.1 GeV, and suggest a minimum or a shoulder in the vicinity of 1.8 GeV. The solid curve represents

the fit of $-\Delta\sigma_L(np)$ from the SP03 solution of the energy dependent (ED) phase shift analysis (PSA) [75] below 1.3 GeV. Above 0.6 GeV the PSA fit is only in qualitative agreement with the measured values. The ANL-ZGS pn data [52] are not shown, but their energy dependence roughly follows the free neutron results.

In Fig. 7 are presented the values of the isosinglet $I = 0$ part of $-\Delta\sigma_L$. They are calculated from the np results and from the averaged pp data, using Eq. (21b). The data point symbols are as in Fig. 6. Since the pp data are accurate, the $-\Delta\sigma_L(I = 0)$ values have approximately two times larger errors than the np results. For this reason, an improved accuracy of np measurements is important. The Dubna results show a plateau around 1.4 GeV, followed by a fast decrease and suggest a minimum in the vicinity of 1.8 GeV. This structure is better pronounced than the similar one in the $-\Delta\sigma_L(np)$ energy dependence (Fig. 6). The solid curve was calculated from np and pp ED PSA predictions below 1.3 GeV ([75] solution SP03). Above 0.5 GeV the PSA solution is not in agreement with the data.

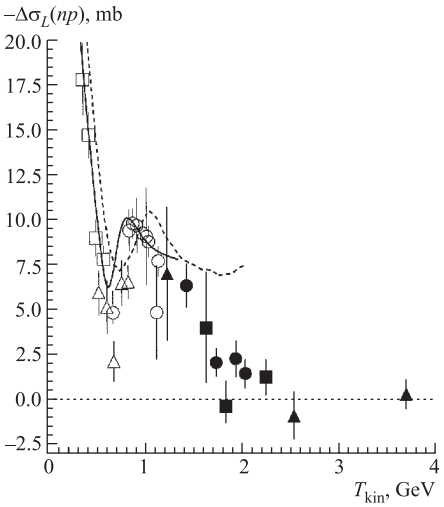

Fig. 6. Energy dependence of $-\Delta\sigma_L(np)$. ● — JINR [70]; ▲ — JINR [66, 67]; ■ — JINR [68, 69]; □ — PSI [56]; △ — LAMPF [57]; ○ — Saturne II [53, 54]; solid curve — ED PSA [75] (SP03 solution); dashed curve — meson-exchange model [76]

Some dynamic models predicted the $-\Delta\sigma_{L,T}$ energy behaviour for np and pp interactions. Below 2.0 GeV, a usual meson exchange theory of NN scattering [76] gives the $-\Delta\sigma_L(np)$ energy dependence as shown by the dashed curve in Fig. 6. It can be seen that this model provides only a qualitative description at low energies and disagrees considerably with the data above 1 GeV.

The investigated energy region corresponds to a possible generation of heavy dibaryons with masses $M > 2.4$ GeV (see review [77]). For example, the model [78, 79] predicts the formation of a heavy dibaryon state with a color octet–octet structure.

The possible manifestation of exotic dibaryons in the energy dependence of different pp and np observables was predicted by another model [80–84]. The authors used the Cloudy Bag Model and an R-matrix connection to long-range meson-exchange force region with the short-range region of asymptotically free quarks. This hybrid model gives the lowest lying exotic six-quark configurations in the isosinglet $^3S_1$ state with the mass $M = 2.63$ GeV ($T_{\rm kin}(n) = 1.81$ GeV).

It is close to the energy, where the structure is suggested by the Dubna results.

Unfortunately, the observed minimum in the energy dependence of $-\Delta\sigma_L(np)$ near 1.8 GeV (see Fig. 6) is only a two standard deviations effect. The same statement holds for the $-\Delta\sigma_L(I=0)$ energy dependence (Fig. 7).

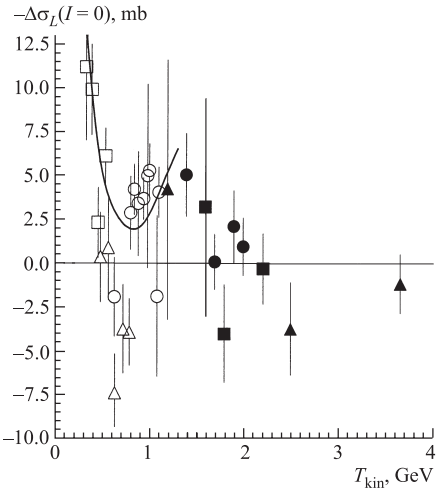

Fig. 7. Energy dependence of the $-\Delta\sigma_L(I=0)$ calculated from the measured np data and the corresponding pp values from [75], solution SP03. The np data at the same energies as in Fig. 6 are used and the $I=0$ results are labeled by the same symbols. The solid curve is calculated from the common np and pp ED PSA [75] (SP03 solution)

The new «perpendicular» superconducting holding coils give the possibility of determining the $-\Delta\sigma_T(np)$. These data are needed to determine the imaginary parts of the forward scattering amplitudes.

An important part of the programme is a determination of the real parts of the $I=0$ and np forward amplitudes. We assume, that the $I=1$ complex amplitudes are known at any angle, whereas the imaginary parts of $I=0$ amplitudes are known in the forward direction. Symmetry conditions, shown in Table 1, connect the amplitudes a to e in Eq. (12) at $\theta_{\rm cm}$ and $\pi-\theta_{\rm cm}$ for the given pure isospin states $I=0$ and $I=1$ [38,41].

Table 1. **Symmetry properties of the NN-scattering amplitudes**

$I=0$ amplitudes	$I=1$ amplitudes
$a_0(\theta)=+a_0(\pi-\theta)$	$a_1(\theta)=-a_1(\pi-\theta)$
$b_0(\theta)=+c_0(\pi-\theta)$	$b_1(\theta)=-c_1(\pi-\theta)$
$c_0(\theta)=+b_0(\pi-\theta)$	$c_1(\theta)=-b_1(\pi-\theta)$
$d_0(\theta)=-d_0(\pi-\theta)$	$d_1(\theta)=+d_1(\pi-\theta)$
$e_0(\theta)=-e_0(\pi-\theta)$	$e_1(\theta)=+e_1(\pi-\theta)$

Using Table 1, the Im Ampl$(I=0)$ forward amplitudes can be easily transformed onto the backward direction, where Im Ampl(np) are determined from Eqs. (20). As mentioned above, to reconstruct unknown Re Ampl(np) at $\theta = 0^\circ$ one needs at least three other observables. The amplitude symmetries allow one to carry out np measurements in the experimentally accessible backward direction. The scattering observables are bilinear combinations of real and imaginary parts of amplitudes, where each term contains a product of one direct and one complex conjugate amplitude [38,41].

The procedure has been proposed in Ref. 51. The np differential cross section $d\sigma/d\Omega$ at $\theta_{\rm cm} = \pi$ is known in a large energy interval (see review [85]). Two other observables could be spin-correlation parameters $A_{00nn}(np)$ and $A_{00kk}(np)$, both measured in a single elastic inclusive scattering. The observables are related to scattering amplitudes as

$$\frac{d\sigma}{d\Omega} = \frac{1}{2}\Big(|a|^2 + |b|^2 + |c|^2 + |d|^2 + |e|^2\Big), \tag{24}$$

$$\frac{d\sigma}{d\Omega}\, A_{00nn} = \frac{1}{2}\Big(|a|^2 - |b|^2 - |c|^2 + |d|^2 + |e|^2\Big), \tag{25}$$

$$\frac{d\sigma}{d\Omega}\, A_{00kk} = -\mathrm{Re}\, a^* d\ \cos\theta + \mathrm{Im}\, d^* e\ \sin\theta + \mathrm{Re}\, b^* c. \tag{26}$$

In the backward direction $e = 0$ (Eq. (14b)) and the corresponding terms vanish. Equation (26) gives $(d\sigma)/d\Omega)\ A_{00nn} = \mathrm{Re}\, a^* d + \mathrm{Re}\, b^* c$, since $\cos\pi = -1$ and $\sin\pi = 0$. Using simple relation of the type

$$|a+d|^2 = |a|^2 + |d|^2 + \mathrm{Re}\, a^* d, \tag{27}$$

together with (14b) one finds

$$\frac{d\sigma}{d\Omega}\ (1 + A_{00kk}) = (b+c)^2, \tag{28}$$

$$\frac{d\sigma}{d\Omega}\ (1 - A_{00kk} - 2A_{00nn}) = (b-c)^2, \tag{29}$$

$$\frac{d\sigma}{d\Omega}\ (1 - A_{00kk} + 2A_{00nn}) = (2d-b-c)^2, \tag{30}$$

where all quantities are taken at $\theta_{\rm cm} = \pi$. Three remaining real parts will be determined with an independent sign ambiguity for each amplitude combination and, therefore, DRSA at one energy gives eight possible solutions. Any other independent nonzero observable, or an additional constraint, decreases the global ambiguity by a factor of two [51]. Finally, at $\theta_{\rm cm} = \pi$, Re Ampl$(I=0)$ are deduced, transformed onto the forward direction, where Re Ampl(np) are reconstructed using again Eq. (20).

The $\Delta\sigma_L$ setup was completed by an apparatus, allowing the measurement in the backward direction. Spin-correlation parameters can be measured simultaneously with the $\Delta\sigma_{L,T}$ experiments. The test-runs, using the unpolarized beam and target provided encouraging results.

A complete DRSA would allow one to discuss possible energy-dependent structures on the level of complex scattering amplitudes and not only on the level of observables.

2.2. DELTA Experiment. The aim of this experiment using the new DELTA setup is a search for the spin-dependent phenomena of π^0- and η-meson production in NN collisions with a polarized nucleon beam and PPT at energies up to 2.5 GeV. The responsible person is V. A. Krasnov.

Table 2. **Properties of π^0 and η mesons**

Parameters	Particles	
	π^0	η
J^{PC}	0^{-+}	0^{-+}
(I, I_3)	(1, 0)	(0, 0)
Quark w.f.	$(u\bar{u} - d\bar{d})\sqrt{2}$	$(u\bar{u} + d\bar{d} - 2s\bar{s})\sqrt{6}$
Mass, MeV	134.9	548.8
Mean life, s	$0.83 \cdot 10^{-16}$	$0.75 \cdot 10^{-18}$
2γ decay fraction, %	98.8	39

Properties of π^0 and η mesons are given in Table 2. Both mesons are members of the pseudoscalar meson nonet and their spins, parity and G parity are identical. A major difference is in their isospin and quark wave function, since η also contains a $s\bar{s}$ pair, reflecting its relative large mass. An attractive feature of the η meson is a selective excitation of the $N^*(1535)$ S_{11} resonance in ηN interaction close to the production threshold.

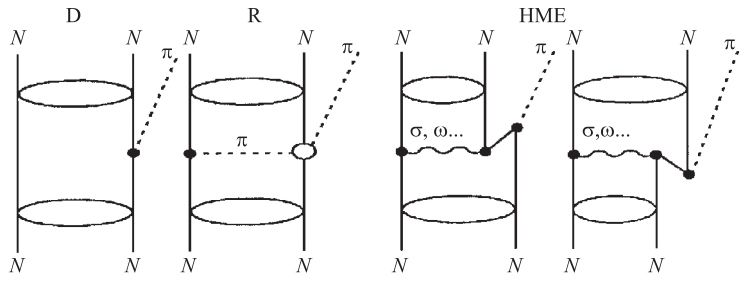

Fig. 8. Pion production mechanisms included in the model: D — direct pion emission; R — pion rescattering and HME — heavy meson exchange

The reaction $NN \to NN\pi$ is the dominant NN inelastic process in the energy region under discussion. Since the pion can rescatter on the nucleon before its emission, it could be used to study the off-shell properties of πN interactions. Furthermore, the reactions $NN \to NN\pi$ check meson production models for such heavier mesons as σ and ω (see model calculation in Fig. 8). The role of different pion production mechanisms can be investigated in inelastic reaction with polarized nucleons, including $np \to d\pi^0$ [86].

No experimental data for η-meson production with polarized nucleons are available yet. Existing data concern mainly the total cross section energy dependence for neutral meson production [87, 88]. Neverheless, these experiments are interesting, since:

• A high momentum transfer (~ 1 GeV) to the nucleon takes place in these processes.

• An unexpected strong energy dependence of η-meson production was observed near the threshold [89].

• The question of nucleon strangeness rises [90].

A possible existence of hidden strangeness in the nucleon has recently become one of the most controversial problems in nuclear and hadron physics. The polarized deep-inelastic lepton-proton scattering experiments (EMC, NMC, SMC, SLAC-E143) indicate a significant role of strange sea quarks in the nucleon structure [91]. Therefore, it would be interesting to study the process of η-meson production in pp and np collisions with polarized nucleons [93]. Measurements of some two-spin observables in pp and np collisions may be very sensitive to the hidden strangeness content of nucleons. The determination of a relative spin-singlet and spin-triplet amplitude contributions may result in a model-independent theoretical analysis of the problem.

To study π^0 and η production, the DELTA lead-glass Cherenkov spectrometer has been designed to determine the energies and outgoing angles of γ quanta from meson decay in the target (Fig. 9). The spectometer is completely assembled. It consists of two blocks, each containing 150 lead-glass prisms, and of a 14 layer scintillation telescope (opto-fiber plates) for multi-ΔE measurements of charged particles. The detectors may be adjusted or rotated in the vertical and horizontal planes by remote computer control.

At least a part of the DELTA experiment could run simultaneously with the measurement of $-\Delta\sigma_T(np)$ (Subsec. 2.1). Different tests were perfomed in 2001 and first results were presented.

NIS Project. A similar project NIS was proposed by VBLHE and the JINR Laboratory of Particle Physics (LPP). The aim is a search for nucleon strangeness, including violation of the OZI rule in the vector meson production. It is necessary to carry out measurements of the production cross sections of ϕ and ω mesons near their production threshold in nucleon interactions, i.e., at laboratory nucleon momenta above 2.7 GeV/c (see [92]). Responsible person is E. A. Strokovsky.

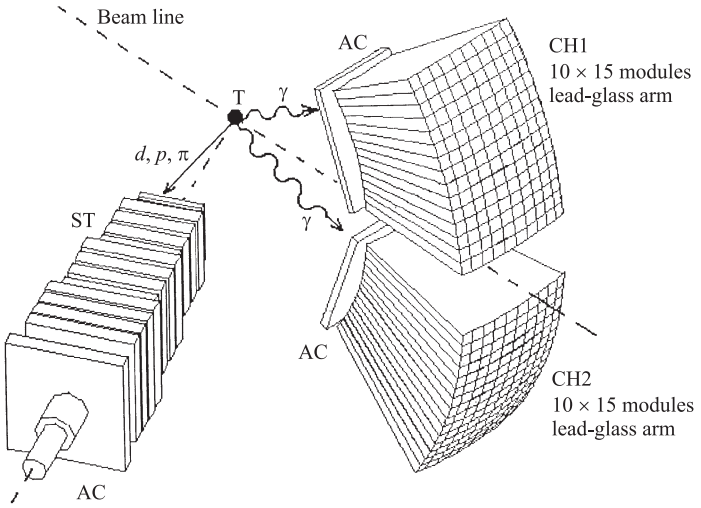

Fig. 9. A schematic view of the DELTA detector positions: T — polarized proton target PPT; CH1, CH2 — two arms of the Cherenkov lead-glass spectrometer for two gammas after neutral meson decay measurements; ST — 14-layer fiber-optics scintillation telescope for multi-ΔE measurements of charged particles; AC — anticoincidence detectors

2.3. pp **SINGLET Experiment.** Throughout Subsec. 2.3 the four spin-index notation and formulae from Subsec. 2.1 are used [38]. The aim of the experiment is the measurement of the energy dependence of the spin correlation parameter A_{00nn} in quasi-elastic pp scattering at angles close to $\theta_{\rm cm} = 90^\circ$. The proton kinetic energy values will cover an interval of a few hundreds MeV around

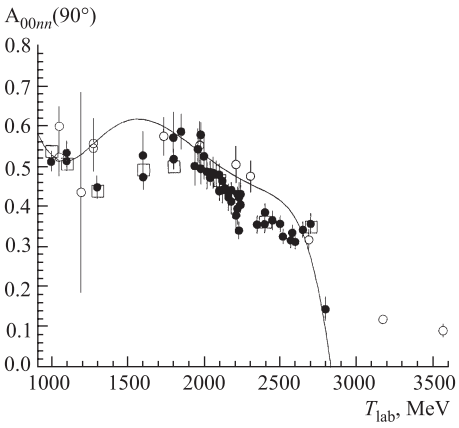

Fig. 10. The distribution of $A_{00nn}(90^\circ)$: ● — Saturne II data [94]; ○ — other data; □ — Saclay–Geneva PSA sol. 2001 [50]; solid curve — ED PSA [96] sol. WI00

2.8 GeV. The beam and target polarizations are oriented vertically, and vertical holding coils for MPT are needed. The person responsible for the experiment is E. A. Strokovsky and the spokespersons are E. A. Strokovsky and N. M. Piskunov. A part of the apparatus for this experiment was succesfully tested in 2001.

This experiment was triggered off by a surprising behaviour of the $A_{00nn}(90^\circ)$ energy dependence, observed around 2.8 GeV at Saturne II, close to the energy limit of the accelerator [95]. Accurate measurements between 2.35 and 2.70 GeV in small energy steps show roughly constant values of $A_{00nn}(90^\circ) \sim 0.35$. When increasing the beam energy to 2.8 GeV, the $A_{00nn}(90^\circ)$ value dropped down by a factor of 3 within a small energy interval. From the existing ANL-ZGS data, measured at several higher energies, it follows that $A_{00nn}(90^\circ)$ remain on the level of 0.1 up to ~ 7 GeV. This is shown in Fig. 10, where, in addition, the predictions of ED PSA [96] and the fixed energy (FE) Saclay–Geneva PSA sol. 2001 [50] are plotted.

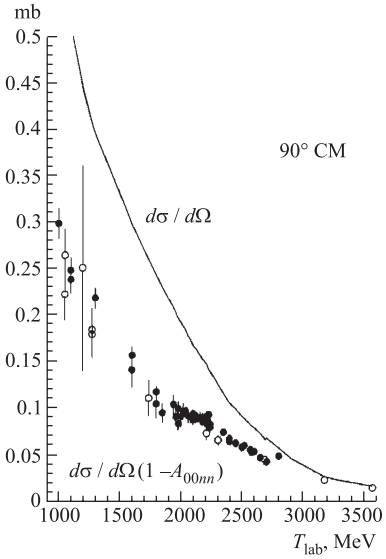

Fig. 11. The spin-singlet amplitude reconstruction: ● — Saturne II data [94]; ○ — other data

The differential cross section $d\sigma/d\Omega$ is known and A_{00nn} is measured in the single scattering exclusive experiment. Both observables are symmetric with respect to $\theta_{\rm cm} = 90^\circ$. Taking the scattering matrix in the form of Eq. (12), the two observables are expressed in terms of the scattering amplitudes given in Eqs. (24) and (25).

Subtracting (25) from (24) gives

$$\frac{d\sigma}{d\Omega}(1 - A_{00nn}) = |b|^2 + |c|^2. \tag{31}$$

Using Table 1 for $I = 1$ and $\theta_{\rm cm} = 90^\circ$, in *pp* scattering only three amplitudes survive:

$$a = 0,\ b = -c,\ d \neq 0,\ e \neq 0. \tag{32}$$

The simple relation at this angle

$$\frac{d\sigma}{d\Omega}(1 - A_{00nn}) = 2\ |b|^2 = |A_S|^2 \tag{33}$$

gives the pure spin-singlet scattering amplitude $|A_S|^2$. DRSA as a function of energy for all measured data is shown in Fig. 11. One observes a clear

narrow local maximum at 2.8 GeV. It is worth checking its position and width in a dedicated counter experiment, since one of the possible explanations of this anomaly is a spin-singlet resonance behaviour.

The importance of the measurement is supported by the fact that the angular dependences of A_{00nn} at 2.7 and 2.8 GeV are totally different. This is demonstrated by Fig. 12, *a, b*.

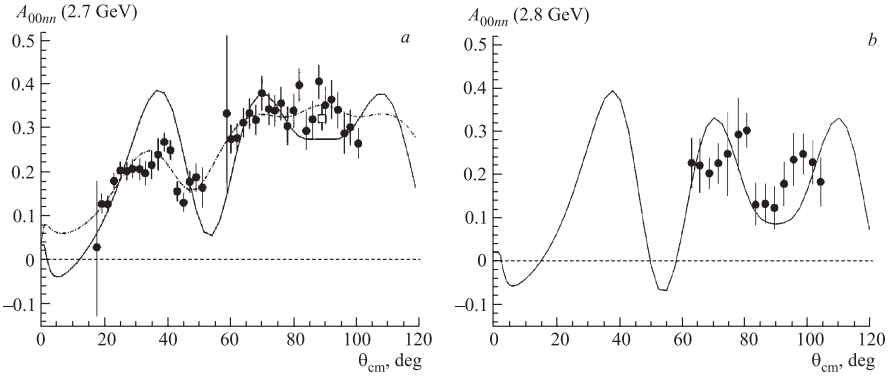

Fig. 12. The angular dependences of A_{00nn} at 2.7 (*a*) and 2.8 GeV (*b*): ● — Saturne II data [94]; dashed curve — Saclay–Geneva PSA sol. 2001 [50]; solid curve — GW/VPI PSA sol. WI00 [96]

3. INVESTIGATION OF DEUTERON STRUCTURE

In this and following sections mainly the experiments using deuteron polarized beams and unpolarized targets are treated.

It is well known that nucleons have an internal structure, that they can be excited to a resonance and that they are extended objects. This means that the standard «nucleonic» picture of nuclei is not self-consistent and contains internal contradictions. To avoid these contradictions, one must take into account the compositeness of the nucleons and their quark structure when the relative momenta are high enough, i.e., the relative distances are short.

Applying the Pauli principle on the level of the nucleon quark structure, in any consistent description of the nuclear structure at short distances the compositeness of nucleons is to be taken into account. This was stressed, e.g., by Kobushkin [97, 98]. A large amount of spin-dependent data, which are very sensitive to the nonstandard content of nuclei, provide strong arguments that the composite nature of nucleons cannot be ignored starting from relative momenta of $\sim$ 200–300 MeV/c. Such data come from deuteron break-up experiments and from backward elastic dp scattering (see below).

3.1. Deuteron Break-Up in Collinear Kinematics. The key feature of these experiments was collinear kinematics, i.e., spectra of proton-fragments were studied at 0° (in the direction of the incident beam). The proton momentum region was from $p_d/2$ (the most probable proton momentum) up to the maximal possible which corresponds to the limit of the backward elastic dp scattering. In this kinematics, the shape of the spectra is determined mostly by the wave function of the studied nuclei [97, 99–102]. Strong disagreement between the data on inclusive differential cross sections and theoretical models of the reaction mechanism, which make use of standard nucleon–proton wave functions (WF) of the probed nuclei, was observed in all experiments. It is demonstrated in Fig. 13, *a*, where the «empirical momentum density» (EMD) distribution of protons in the deuteron, extracted from the inclusive cross sections of $d + p \to p + X$, is shown [101, 102, 105, 106]. It is plotted together with similar data from $e + d \to e' + X$ reaction [107]. An excellent agreement of the hadronic and electromagnetic probes clearly demonstrates that the type of probes is irrelevant.

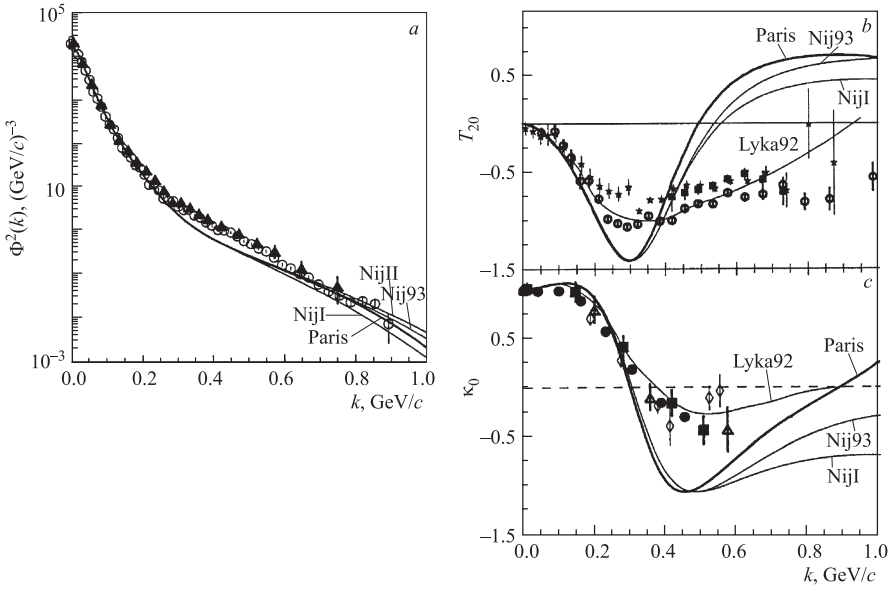

Fig. 13. World data for deuteron break-up on protons and carbon nuclei. The Empirical Momentum Density (EMD), denoted here as Φ^2, is defined in the text. Lines are calculated in the quasi-impulse approximation with different models for the deuteron wave function (DWF) (labels «Paris», «Nij93», «NijI» for the Paris and Nijmegen DWFs) and in the model where rescattering effects and final state interactions are taken into account («Lyka92»[103, 104]). *a*) ○ — H$(d,p)X$ (Dubna); ▲ — $d(e,e')X$ (SLAC); *b*) ★ — C$(d,p)X$ (Dubna, 1988); ○ — $p(d,p)X$ (Dubna, 1994); ■ — C$(d,p)X$ (Dubna, 1995); *c*) ● — Saclay (1991); ■ — ALPHA (1992); ◇ — ANOMALON (1993); △ — ALPHA (1994)

The EMD is related to the invariant cross section $E_p\ d^3\sigma/d\mathbf{p}$:

$$E_p\ \frac{d^3\sigma}{d\mathbf{p}} \sim \Phi^2(k)\frac{1}{4(1-\alpha)}\sqrt{\frac{m_p^2+p_\perp^2}{\alpha(1-\alpha)}}F(N,d)\frac{E_p}{d\mathbf{p}}, \tag{34}$$

$$\alpha = \frac{p_{||}+E_p}{p_d+E_d};\ k_\perp = p_\perp;\ k = \sqrt{\frac{m_p^2+p_\perp^2}{4\alpha(1-\alpha)}-m_p^2}. \tag{35}$$

Here $d\mathbf{p} = dp_x dp_y dp_z$; Φ is the EMD; k is the Light Cone Dynamics (LCD) variable (see, e.g., [97, 99, 100]); p is the momentum of the proton-fragment, with the perpendicular ($p_\perp$) and the longitudinal ($p_{||}$) components relative to the initial beam momentum direction; m_p is the proton mass; E_p, and E_d are the total energies of the detected proton and the initial deuteron, respectively. The factor F is the so-called kinematical «flux factor», which guarantees that outside the kinematic limits the cross sections are zero. It can be written as the ratio of the kinematic «triangle functions» $\sqrt{\lambda(a,b,c)}$, where a is the mass of the target nucleus squared $\mathrm{M}^2_{\mathrm{targ}}$, b is either the averaged nucleon mass squared (m_N^2), or the corresponding quantity for the deuteron ($4m_N^2$). Finally, c is the total energy squared, s_N or s_d in the CM systems «$N+$ target nucleus» or «$d+$ target nucleus».

In the experiments with polarized deuteron beams, new observables were measured in the same kinematics, namely, the tensor analyzing power (T_{20} or A_{yy}) and the coefficient of the polarization transfer (κ_0) from the vertically polarized deuterons to the proton-fragments. The measurements were done in the entire available interval of the polarized deuteron momenta, from few GeV/c up to 9 GeV/c. This made it possible to probe the deuteron structure up to the relative momenta of the nucleon constituents close to 1 GeV/c (relative internucleon distances as small as $\sim 0.2{-}0.3$ fm). Summary of these data is presented in Figs. 13, *b, c*. The tensor analyzing power T_{20} was reported in Refs. 74, 108–114; coefficient of the polarization transfer κ_0, in Refs. 73, 74, 108, 109, 115, 116. The experiments were done mostly in Dubna and in Saclay. The JINR experiments were performed at ALPHA and ANOMALON [118] arrays, recently at the SPHERE [34, 35] installation as well [119].

The recent predictions are plotted. Former predictions were given, e.g., in Ref. 120. A strong discrepancy between models and data is obvious, only one more or less successful description of all these data within an unified picture is based on the approach, where the Pauli principle on the constituent quark level was taken into account. This approach was developed, e.g., in [121] (see also [97, 98]).

A systematic analysis of the observables carried out in [122] shows, that impulse approximation (IA), multiple scattering (MS) and contribution of quark exchange (QE) are important to explain the existing data. An example concerning

T_{20} data description in the inclusive breakup reactions $^1\mathrm{H}(d,p)$ and $^{12}\mathrm{C}(d,p)$ at $p_d = 9.1$ GeV/c is given in Fig. 14. Exprimental data are from [74, 108, 110, 111].

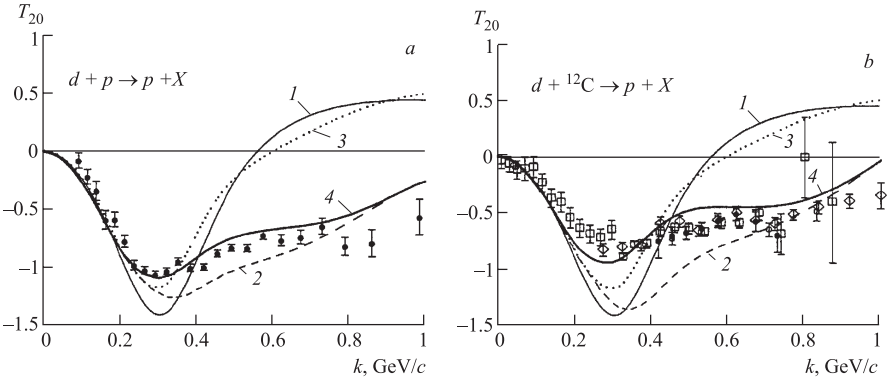

Fig. 14. Tenzor analyzing power, T_{20}, for the 0° inclusive break-up at $p_d = 9.1$ GeV/c plotted versus the relativistic internal momentum in the deuteron k. *a*) $^1\mathrm{H}(d,p)$, ● — [108]. *b*) $^{12}\mathrm{C}(d,p)$, ● — [108]; ○ — [74]; ◇ — [110]; □ — [111]. *1* — IA; *2* — IA + MS; *3* — IA + QE; *4* — IA + MS + QE

Posible measurements of deuteron break-up observables using the polarized beam and PPT were discussed in [123].

KAPPA Project. New measurements of the coefficient of the polarization transfer (κ_0) from the vertically polarized deuterons to protons in the reaction $d + \mathrm{C} \to p + X$ at internal momenta of 0.6–0.8 GeV/c are proposed in project KAPPA. The responsible person is I. M. Sitnik.

3.2. Deuteron–Proton Backward Elastic Scattering. Since this reaction involves large $-t$ values, it may be a good probe for very short distances in the deuteron and it contains information about the short range regime of the 3-nucleon system. The available data for the differential cross section are shown in Fig. 15 [124]. No quantitative description of the energy dependence exists so far above 1 GeV.

EMD of protons in the deuteron can be related with the differential cross section as follows:

$$\frac{d\sigma}{d\Omega} = \frac{3\pi^2}{64s}\frac{\epsilon^2}{(1-\alpha)^2}(4\epsilon^2 - m_d^2)\Phi^4(k);\ 4\epsilon^2 = \frac{m_p^2 + k_\perp^2}{\alpha(1-\alpha)}, \tag{36}$$

$$k_\perp = p\sin(\pi - \theta_{\mathrm{cm}});\quad \alpha = \frac{E_p + p\sin(\pi - \theta_{\mathrm{cm}})}{E_d + p}, \tag{37}$$

where p is the CM momentum of the proton–deuteron system. The EMD extracted from the data in Fig. 15 is shown in Fig. 16, *a*.

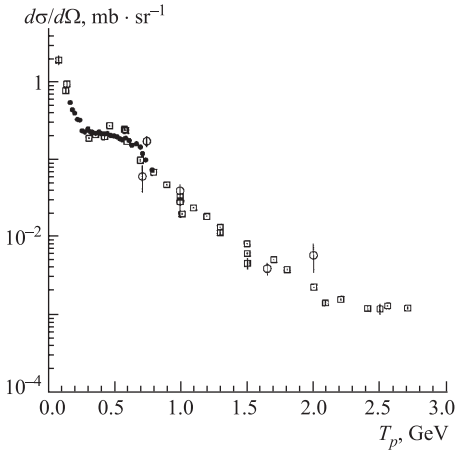

Fig. 15. The differential cross sections for $p(d,p)d$ (□ — world data) elastic scattering, plotted versus initial kinetic energy per nucleon, T_p

Data for T_{20} were obtained in Saclay [27, 28, 125] and in Dubna [126, 127], that for κ_0 were obtained in Saclay only [125]. All these data were measured in the inclusive experiments using detection of recoil protons only (see also review [128]). One Saclay point was obtained from the kinematically redundant experiment at SPES4-π setup, where both scattered deuteron and proton were detected in coincidence and their momenta were measured [129] (see Fig. 17).

Comparing Figs. 13, *a–c* with Fig. 16, *a–c*, one can conclude that the EMDs extracted from $(d,p)X$ break-up and $p(d,p)d$ elastic scatter-

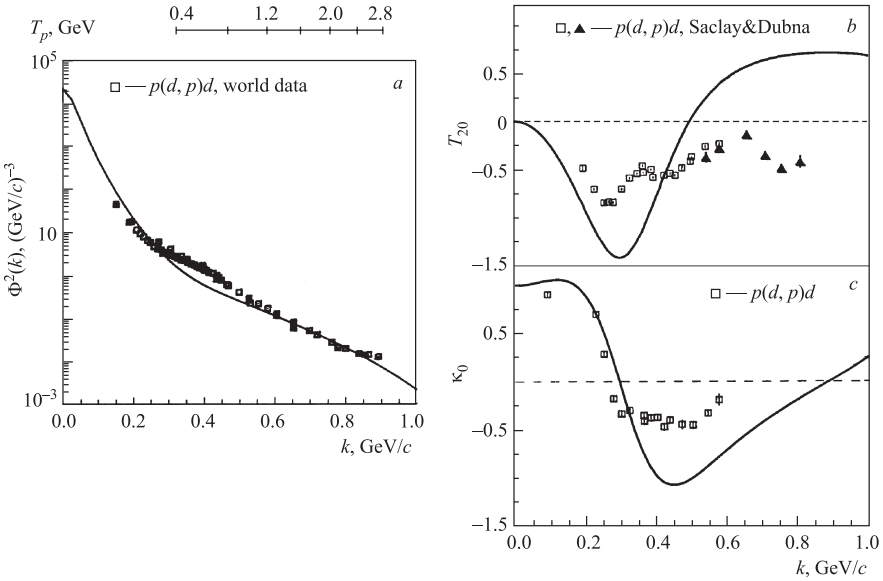

Fig. 16. The summary of the data for backward elastic scattering $p(d,p)d$. The EMD is extracted from the data presented in Fig. 15. Line — One-Nucleon-Exchange (ONE) predictions with Paris DWF. The upper scale illustrates the correspondence between T_p and k

ing coincide unexpectedly well, whereas the spin-dependent observables have rather different k dependence. But, surprisingly, when T_{20} and κ_0 data from these reactions are plotted on the same $T_{20} - \kappa_0$ plot [130], the corresponding trajectories coincide very well. They are far away from the circle

$$\left(T_{20} + \frac{1}{2\sqrt{2}}\right)^2 + \kappa_0^2 = \frac{9}{8}. \quad (38)$$

Equation (38) is valid strictly for «one nucleon exchange» (ONE) [131] and Impulse Approximation (IA) for the $(d,p)X$ and $p(d,p)d$ reactions, if the DWF contains only two orbital momentum states: S and D. If there are more orbital states, e.g., P waves coming from $N - N^\star$ content of the deuteron with negative parity baryonic resonance $N^\star$, the circle will be destroyed. The behaviour of T_{20} as a function of κ_0 is shown in Fig. 18 and remains unexplained.

Intriguing are two structures in the spin-observable energy dependence. One at $k \sim 0.35$ GeV/c was first observed in Saclay [27,28,125], the second one in Dubna [126,127].

Note that it will be hardly possible to extend the electron–deuteron scattering data to high k in order to search for similarities between hadronic and leptonic probes.

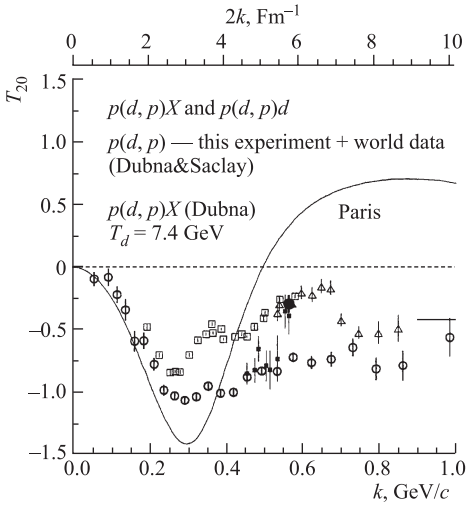

Fig. 17. Comparison of the break-up results and the backward dp elastic scattering data. The black dot is from the Saclay exclusive experiment [29]

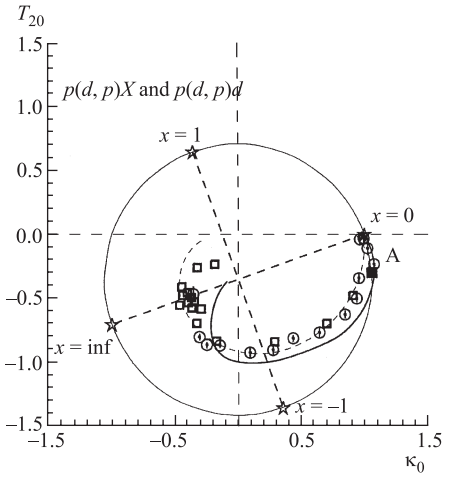

Fig. 18. $T_{20} - \kappa_0$ plot of existing data. The circle is given by Eq. (38)

BES Project. The direct reconstruction of scattering amplitudes (DRSA) for the $dp \to dp$ system is important, similarly as for NN elastic scattering (see Subsec. 2.1). The problem of a complete experiment in backward elastic scattering (BES) was treated in Ref. 132. Existing observables are

insufficient for this purpose and new independent quantities are needed. They could be measured using polarized deuteron beam together with PPT, or using polarized protons scattered on PDT.

Assuming conservation laws, the process of elastic scattering of particles with spins 1 and 1/2 at an arbitrary angle is determined by 12 independent complex amplitudes [133]. DRSA was never perfomed at any energy, and angle, since at most 20 observables were measured at $T_{\rm kin}(d) = 1.6$ GeV [26]. The collinearity conditions, when the total helicity of the interacting particles is conserved, reduces the number of independent amplitudes to 4 [135, 136].

The analysis of the complete experiment has been carried out in terms of a model-independent parametrization of the spin structure of collinear backward dp collisions. Such a formalism is not connected directly either with the deuteron model, or with the reaction mechanism. Of course, the final goal is to connect the determined amplitudes with an adequate model of the deuteron.

The choice of the minimal set of observables, necessary to perform DRSA, can vary depending on experimental conditions. Some observables have already been measured. DRSA of all possible cross-section asymmetries is given in [134]. To calculate some polarization observables DRSA was applied in [135–137], and IA expectations were obtained in [138]. Authors of [132] calculated the complete set of observables, connected with the polarization of one of final particles. Double and triple spin correlations are considered. The IA expectations for the majority of them are given. About fifty observables are possible for BES. This set is strongly overdetermined, but the description of each of the observables helps one to build a reasonable sequence of following measurements. This means a compromise in choosing between the minimal set of observables, or a wider set of less complicated measurements.

Four complex scattering amplitudes are to be determined in the backward direction and, in principle, eight observables are to be measured. A common undetermined phase between the amplitudes decreases the number of observables to seven, but the amplitudes will be relative with respect either to one real, or one imaginary part of one arbitrary amplitude. Since all observables are bilinear function of amplitudes, each amplitude is determined with an independent sign ambiguity. Therefore, DRSA at one energy gives $2^7 = 128$ possible solutions, at most. As is explained in Subsec. 2.1, any other independent nonzero observable, or a constraint, decreases the global ambiguity by a factor of two. Under these conditions, for the direct reconstruction a knowledge of seven additional independent parameters is needed.

Several spin-dependent observables are sensitive to the contribution of P waves in DWF [135–137]. If S wave intersects zero and D wave does not exceed 5%, the effects induced by the P waves could achieve dozens per cent.

The deuteron constituent's internal momenta from 0.2 to 1 GeV/c are the most interesting. The corresponding primary beam momentum range is $0.65{-}4.0$ GeV/c

for a proton beam and deuterium target or $1.3{-}8.0$ GeV/c for a deuteron beam and hydrogen target. As a first step of the BES programme is a measurement of the spin correlation parameter C_{NNOO} in backward elastic dp scattering, when both the initial deuteron and the proton have a transversal (parallel or antiparallel) polarizations. (A diffferent notation is applied then in Subsec. 2.1)

In [132], authors discuss mainly backward elastic dp scattering. The deduced relations are valid also for backward elastic $^3\mathrm{He} - d$ scattering, or for any other reaction with the same spin structure. Responsible person for the BES programme is I. M. Sitnik, the spokespersons are I. M. Sitnik and L. S. Azhgirey.

3.3. Deuteron Break-Up in Noncollinear Kinematics. The data on A_{yy} in the deuteron inclusive break-up reactions of 9 GeV/c deuterons on hydrogen and carbon nuclei were measured in noncollinear kinematics as well [36, 139–141]. In these experiments protons were emitted at $\theta_{\mathrm{lab}} = 85, 130$ and 160 mrad and their transverse momenta up to 900 MeV/c were measured. The SPHERE [34,35] setup was used. In Fig. 19, the data obtained at $\theta_{\mathrm{lab}} = 85$ mrad are compared to the data measured at $\theta = 0$ and to different model predictions. The data indicate a significant dependence of A_{yy} on the transverse momenta, what contradicts the calculations using standard DWF.

Two other projects of experiments in this domain exist.

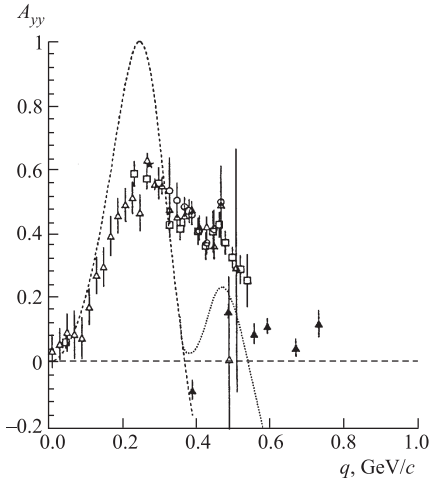

Fig. 19. A_{yy} data at $\theta_{\mathrm{lab}} = 85$ mrad (▲) compared with the data obtained at 0° on carbon target: △ — [111, 117]; □ — [110]; ○ — [108]; q is the proton momentum in the rest frame of the deuteron. The dashed and dotted lines are the results of calculations using Paris DWF for 0 and 85 mrad proton emission angles, respectively

LNS Project. In the experimental programme «Light Nuclei Structure» (LNS) it is planned to investigate deuteron and ^{3}He structure at small distances between nucleons. The programme includes the study of dp elastic scattering and deuteron break-up reactions in dp interactions, using unpolarized and polarized deuteron beams, the internal target station of the Nuclotron (see Sec. 1) and measurements of the tensor analyzing power of the reactions $d + d \to n +$ ^{3}He or $d + d \to$

$p +\ ^3$H. The programme represents the collaboration VBLHE–RIKEN (Japan). Responsible JINR person is V. P. Ladygin.

PHe3 Project. The experiment «Probing Short-Range Spin Structure of Deuteron with Polarized Deuteron Beam and Polarized ^{3}He Target» (PHe3) is the joint VBLHE–RIKEN project. The structure of ^{3}He and ^{3}H will be studied at distances, unachievable now with the use of lepton probes. Angular dependences of the tensor analyzing powers A_{yy}, A_{xx}, and A_{xz} in the reactions $d + d \to n +\ ^3$He and $d + d \to p +\ ^3$H will be measured. These polarization observables are sensitive to the neutron (proton) distribution in ^{3}He (^{3}H) at small distances in the framework of ONE approach [131]. Since ^{3}He and ^{3}H are mirror nuclei with respect to the number of protons and neutrons, the difference in observable values can be interpreted in terms of charge symmetry violation.

In the polarization correlation measurements, the spin-exchange-type polarized ^{3}He target, developed at RIKEN will be used. The size of the target cell is 5 cm in diameter and 30 cm in length along the beam path. T_{20} is planned to be measured at four energies between 1.0 and 1.75 GeV and the spin correlation parameter at three energies. Responsible JINR person is V. P. Ladygin, spokespersons are A. I. Malakhov and T. Uesaka.

4. SPIN-DEPENDENT OBSERVABLES IN CUMULATIVE REGION

The study of cumulative particle production (CPP) has been carried out in Dubna and at other laboratories from the beginning of the 1970th years [142–152]. As usual, by cumulative particles are meant the particles produced in the fragmentation region of one of the colliding particles beyond the kinematic limit of free NN collisions [147, 148]. The study of cumulative reactions gives information about a high momentum component in fragmenting nuclei. Such an internal momentum corresponds to small internucleonic distances (~ 0.1 fm) at which a manifestation of non-nucleon degrees of freedom in nuclei could be expected [153–156].

In deep inelastic scattering of leptons this internal momentum corresponds to $x_{\mathrm{Bjork}} \geqslant 1$, where the cross sections are too small. From this point of view the hadronic probes are preferable.

4.1. Analyzing Power for Cumulative Proton Production. The first JINR «spin-dependent cumulative» experiment [157] measures the analyzing power in reactions involving emission of fast protons in the interaction of vector polarized deuterons with carbon nuclei. The inclusive reaction $d + \mathrm{C} \to p + X$ was studied at energies 0.6, 0.8, 1.0, and 2.1 GeV/nucleon. A correlation of the two outgoing protons in the reaction $d + \mathrm{C} \to p + p + X$ was investigated at 0.8 GeV/nucleon.

Inclusive measurements of A_y^p were carried out in the internal beam of polarized deuterons, intersecting a thin polyethylene target. The fast protons were

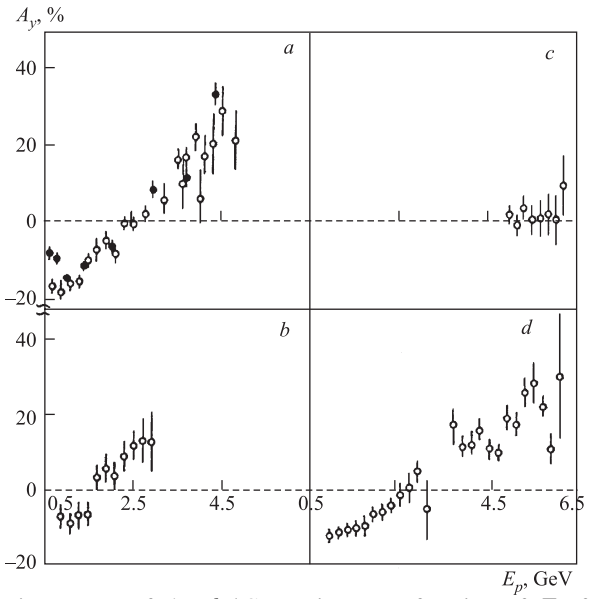

Fig. 20. Analyzing power of the d ↑C reaction as a function of E_p for $\theta_{\rm lab} = 75°$: *a*) $E_d = 0.8$; *b*) 0.6; *c*) 2.1; *d*) 1.0 GeV/nucleon [157]

detected by telescopes of scintillation detectors at several angles. The detectors could identify protons, deuterons and pions. The results at $\theta_{\rm lab} = 75°$ are shown in Fig. 20.

Figure 21 shows values of $A_y^p(75°)$ as a function of the variable $Q = x_C = M_{\rm eff}/m_p$. Here $M_{\rm eff}$ is the mass of the target (at rest), at which the incident proton would have to be scattered elastically in order to be detected with the given momentum, m_p is the proton mass. Q or x_C is called a «cumulative number» in different papers. It can be considered as a number of the target nucleons simultaneously interacting with the incident deuteron. We see that the data for all deuteron energies conform well to a common curve. This agreement may evidence that scattering by heavy clusters is contributing substantially in this kinematic range.

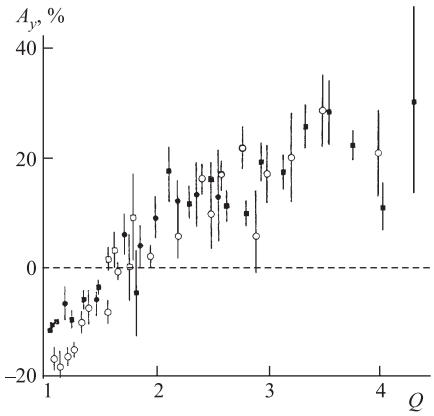

Fig. 21. Analyzing power of the d ↑C reaction as a function of the «cumulative number»: ● — 0.6; ○ — 0.8; ■ — 1.0; □ — 2.1 GeV/nucleon

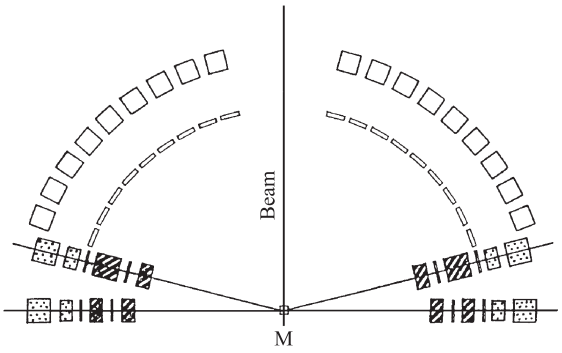

Fig. 22. Setup for the correlation experiment. Open rectangles — plastic scintillators; hatched rectangles — moderators; dotted rectangles — NaI(Tl) crystals

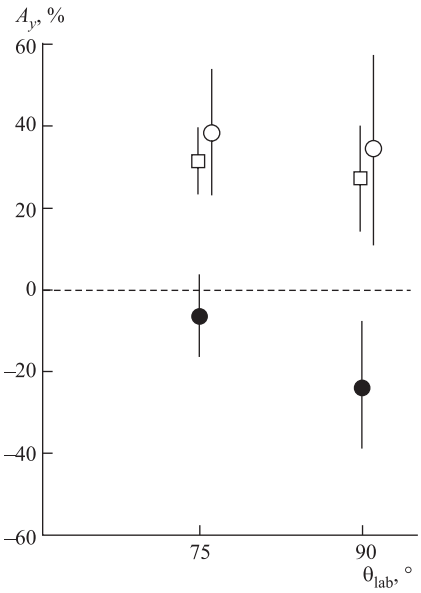

Fig. 23. Analyzing power of the reaction $d\uparrow \mathrm{C} \to p(p,d) + X$ for angles of 75 and 90°, and for various angles of the particles emitted forward. □ — data for a «cumulative» proton in coincidence with a slow proton (the kinetic energy is from 0.04 to 0.22 GeV); ○ — in coincidence with a slow deuteron (the kinetic energy is from 0.05 to 0.25 GeV); ● — in coincidence with a fast proton (with energy above 0.22 GeV)

In the «correlation» experiment, coincidences were detected between fast protons, emitted at $\theta_{\mathrm{lab}} = 75$ or 90°, and particles in the forward hemisphere. A reaction in which the «cumulative proton» is accompanied by fast forward proton is usually linked with the mechanism of single pp scattering. For a cumulative proton, the analyzing power is negative. Coincidences with slower protons and deuterons, which are linked with scattering by clusters, give a positive analyzing power. Its value is larger than A_y^p for inclusive measurements (Figs. 22, 23).

4.2. Tensor Analyzing Power for Cumulative Pion Production. The deuteron fragmentation into cumulative hadron is one of the suitable reactions to study the deuteron core structure. The simplest model to describe cumulative hadron production is a direct mechanism. Here a nucleon with a high momentum in the projectile (e.g., in the deuteron), collides against a nucleon in the target nucleus and produces a cumulative hadron, for instance in the $NN \to NN\pi$ reaction [161, 162]. The direct mechanism model predictions are in contradiction with the Dubna results [158–160]. These experiments, measuring the tensor analyzing power T_{20} for cumulative pion production will be treated together. The results concern following investigations in the forward direction:

• Study of the reaction $d + \mathrm{C} \to \pi^-(0^\circ) + X$ at six incident polarized deuteron momenta ($p_d = 6.2, 6.6, 7.0, 7.4, 8.6, 9$ GeV/c) and the same reaction with positive outgoing pions at 7.4 and 9 GeV/c. The pion momentum was fixed to 3.0 GeV/c at all energies.

• Reaction $d + A \to \pi^-(0^\circ) + X$ at $p_d = 9$ GeV/c using H, Be, and C targets. The pion momenta from 3.5 to 5.3 GeV/c were measured.

The cumulative variable x_C for the cumulative pion production in the reaction $A + B \to \pi + X$ can be written as:

$$x_C = \frac{p_B p_\pi - m_\pi^2/2}{p_A p_\pi - m_N^2 - p_A p_\pi}, \tag{39}$$

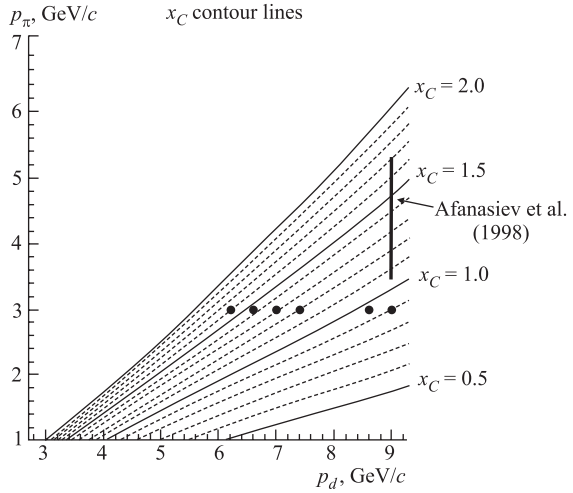

Fig. 24. x_C for the reaction $d + {}^{12}\mathrm{C} \to \pi^\pm + X$ as a function of the momenta of the deuteron and the pion. The black dots and the full line indicate the measured momenta combinations in [159] and [160], respectively

where $p_A,\ p_B$ are the four-momenta per nucleon for projectile and target nuclei, respectively; p_π is the four-momentum of the produced pion; m_N and m_π are the nucleon and pion masses.

The x_C interval extends up to the mass number of the fragmenting nucleus. When the hadron with $x_C > 1$ is produced, it is considered as a cumulative hadron. The backward elastic scattering $dp \to pd$ is a special case of cumulative reactions, when x_C=2. Figure 24 shows x_C for the d+C $\to$ $\pi^-(0^\circ)$+X reaction as a function of the deuteron and pion momenta. The black dots indicate the momentum combination in the experiment [159], the vertical line is the x_C region of [160].

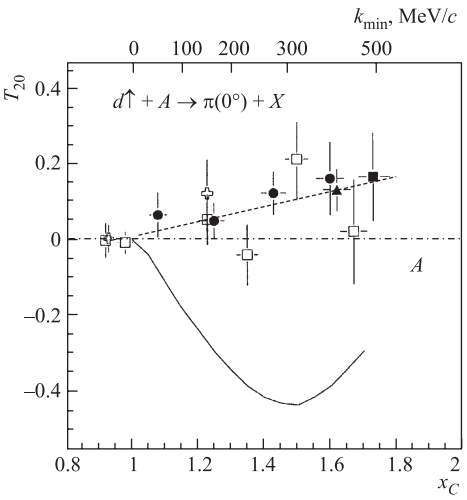

Fig. 25. T_{20} vs. x_C and $k_{\min}$ (see text) for the reaction $d + \mathrm{C} \to \pi^\pm(0^\circ) + X$ at the fragmentation of 9 GeV deuterons on the hydrogen (●), beryllium (▲) and carbon (■, □, ◇) targets [159,160]. The dashed curve is a linear fit of the data ($\chi^2/\mathrm{DF} = 0.5$); the solid curve is the calculation from [159] based on the Paris DWF [163]

In the framework of the direct mechanism, the cumulative hadron is produced by a nucleon with a high internal momentum k in the fragmenting nucleus. Hence, the minimum momentum of the nucleon, $k_{\min}$, which is wanted for cumulative hadron production can be related to x_C: $k_{\min}$ increases from 0 as x_C increases from 1. The T_{20} results from both experiments are plotted in Fig. 25 vs. the variables x_C and $k_{\min}$.

The T_{20} values in the pion production were found to be independent of the target mass number. Although a weak target dependence was seen in the inclusive cross sections for cumulative hadron production [146, 164], it is evident that T_{20} is predominantly determined by the internal structure of the fragmenting deuteron.

The internucleonic distance r_{NN} decreases with increasing x_C and $k_{\min}$. It was evaluated to be $r_{NN} = 0.4$ fm at $x_C = 1.7$. This internucleonic distance corresponds to a large D-wave contribution to the DWF, and therefore a large value of the tensor analyzing power could be expected. The result of the calculations [159], performed in the framework of the direct mechanism using the Paris DWF [163] is shown in Fig. 25 as a solid curve. One can see that the measured T_{20} have positive values over the whole cumulative region and opposite to those predicted by the calculations.

Note that the results in the noncumulative region agree well with existing data. Figure 26 shows the vector analyzing power as a function of the outgoing pion momentum. The angles of emitted pions are around 90° ([165–167] and 24° [168] (see also Sec. 5).

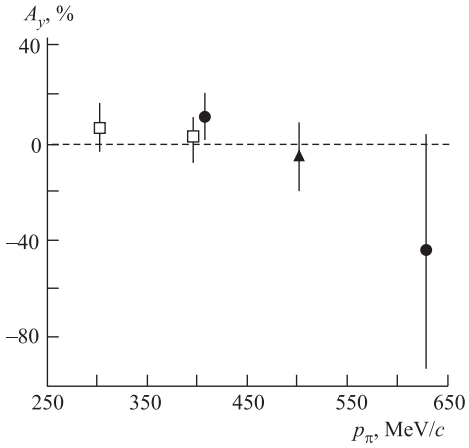

Fig. 26. A_y versus the pion momentum for $d \uparrow + \mathrm{H} \to \pi^{\pm} + X$ reactions at $p_d = 8.9$ GeV/c: ● — $\pi^+(90°)$; ▲ — $\pi^+(78°)$; □ — $\pi^-(90°)$

Two other projects concerning investigations of cumulative particle production exist.

DISK Project. «Study of Cummulative Particles and Structure of the Lightest Nuclei in Experiments with Polarized and Unpolarized Beams» proposes to study the cumulative particle production in deep cumulative region ($x_C \geqslant 3$) and spin effect at lower x_C. The responsible JINR person is Yu. A. Panebratsev and spokespersons are Yu. A. Panebratsev and S. S. Shimansky. The experiment DISK is related with experiments CERES/NA45 and with RHIC STAR.

MARUSIA Project. Project concerns investigations of relativistic multiparticle interactions. The aim is the transition from nucleon to quark-gluon degree of freedom on the basis of the experimental study of hadron production in relativistic nuclear collisions (2–6 GeV/nucleon). In the proposed research the rare subthreshold and cumulative processes will be measured taking into account the polarization of colliding objects. Single-spin asymmetries in the reactions $\uparrow d + A \to \pi^{\pm}, K^{\pm}, p^{\pm} + \ldots$ with simultaneous measurement of centrality and the reaction plane will provide new information on the spin structure of the deuteron. The responsible person is A. A. Baldin.

5. ANALYZING POWERS IN INELASTIC DEUTERON REACTIONS

Inelastic (d, d') scattering on protons and nuclei at various energies offer a possibility of investigating spin-dependent effects in reactions with excitations of baryonic resonances ($\Delta(1232)$, $N^*(1440)$, etc.) Such information in the Δ, Roper and overlapping region, where interference between these resonances might be essential, can help one to understand the properties and underlying mechanism of the reactions studied. It is particularly important for the theory of charge

exchange reactions at intermediate energies. At present the theory is unable to provide a quantitative description of these reactions with nuclei.

Differential cross-section measurements of the deuteron inelastic scattering have been performed in Saclay at 2.95 CeV/c for hydrogen [169, 170], in Dubna for different targets at deuteron momenta up to 9 GeV/c [171–174], and at FNAL [175] at higher momenta for hydrogen. The calculations carried out in the framework of the multiple scattering formalism [174] have shown that the differential cross section of the $\mathrm{H}(d,d')X$ can be satisfactorily described by hadron–hadron double scattering. The amplitudes for the proceses $NN \to NN^*$ have been extracted for $N^*(1440)$, $N^*(1520)$, and $N^*(1680)$ resonances [174].

Spin-dependent experiments measuring T_{20} (or A_{yy}) in (d,d') scattering at the laboratory angles of 0 and $\sim 5^\circ$ on H and C in the p_d interval from 4 to 9 GeV/c were performed during the period from 1994 to 1997. The results are usually presented as functions of the four-momentum transfer squared $-t$ (GeV/c)^2 and an approximately universal behaviour of $T_{20}(t)$ (the scaling) was observed [127, 176, 177] (see Fig. 27).

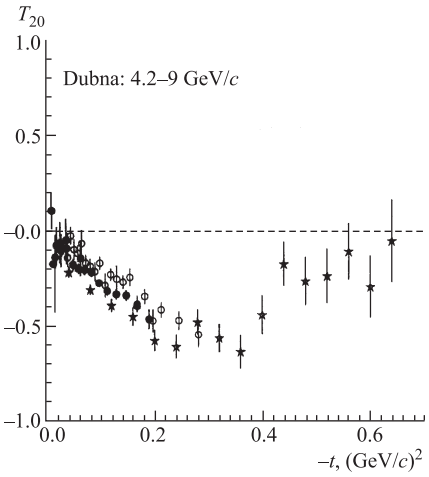

Fig. 27. $T_{20}(t)$ for $p(\vec{d},d')X$. ○ — 4.5 GeV/c [176]; ● — 5.53 GeV/c [176]; ★ — 9 GeV/c [108, 177]

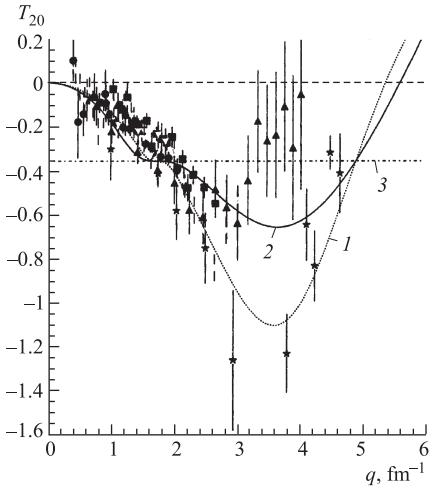

Fig. 28. Comparison of (d,d') and ed scattering: ★ — $ed\,(t_{20})$; ■ — 4.5 GeV/c; ● — 5.5 GeV/c; ▲ — 9 GeV/c; *1* — $r(t)P_{11}$; *2* — $r(t)P_{11} + D_{13} + S_{11}$; *3* — $r(t) = 0$

The experiments have shown a large negative value of T_{20} at $-t \sim 0.3$ (GeV/c)^2. Such a behaviour has been interpreted in the framework of t-channel ω-meson exchange model [178]. Here the cross section and the spin-

dependent observables can be calculated from the known electromagnetic properties of the deuteron and baryonic resonances N^* [179].

The $T_{20}(t)$ data in (d, d') scattering could be compared with the $t_{20}(t)$ results in (e, d) elastic scattering (Fig. 28). In the case of the ω exchange in collinear kinematics $t_{20}(t) \sim T_{20}(t)$. The two quantities are related to the deuteron electromagnetic form factors and to the ratio of the longitudinal over transverse isoscalar form factors of the N^* excitation. It turns out that in the kinematical region under discussion this ratio is nonzero only for $N^*(1440)$ Roper resonance [179].

Note that a measurement of (d, d') inelastic scattering takes few hours, whereas the time needed for ed measurement is two or three orders longer.

A new dimensionless variable with better scaling properties has been proposed in Ref. 180.

$$\Re = \frac{M_x - M_{\rm targ}}{\nu}\ ,\ \nu = \frac{1}{M_{\rm targ}} p_t(p_d - p_{d'}) = m_d u_t(u_d - u_{d'}), \qquad (40)$$

where p_d, $p_{d'}$, and p_t are four-momenta of the projectile, the outgoing deuteron and the target, respectively; u_d, $u_{d'}$, and u_t are their 4-velocities; M_x is the missing mass (final state) and $M_{\rm targ}$ is the target mass (final state). $\Re$ may be interpreted as the ratio of the excitation energy to the full transferred energy, therefore it measures a «degree of inelasticity» of the scattering ($\Re = 0$ is the special case for elastic scattering). Figure 29 shows the $T_{20}(\Re)$ results from Fig. 27.

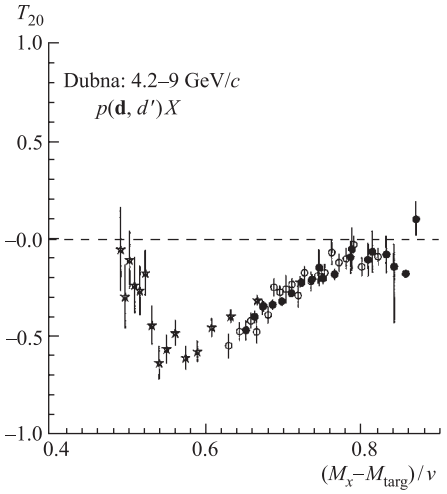

Fig. 29. Data from Fig. 27 plotted versus $\Re$

Spin-dependent experiments measuring the vector and tensor analyzing powers A_y and A_{yy}, respectively, in (d, d') scattering were carried out by the SPHERE [34, 35] collaboration in the vicinity of the low-lying baryons (1440), (1535), and (1650).

The values of the vector analyzing power A_y are small and have large error bars. However the value of A_y in the vicinity of the Roper resonance excitation was found to be 0.155 ± 0.063 [37]. In the framework of the plane-wave impulse approximation (PWIA) such a fact was considered as a significant role of the spin-dependent part of the Roper resonance P_{11}.

Tensor analyzing power A_{yy} was measured at $p_d = 4.5$ GeV/c in deuteron inelastic scattering on beryllium at the laboratory angle of 80 mrad [37] in the

vicinity of baryonic resonances excitation. The results, as a function of the four-momentum transfer t (GeV/c)^2, are in good agreement with the previous data at a zero angle on hydrogen for the deuteron momenta of 4.5, 5.5, and 9 GeV/c [176, 177]. Other results obtained at 9.0 GeV/c on hydrogen (at 0 mrad) and on carbon (at 80 mrad) are reported in Ref. 181. The predictions using DWF for Paris [163] and Bonn potentials [182] are in a complete disagreement with the experimental results.

Within the PWIA approach, A_{yy} does not depend on the elementary amplitude $NN \to NN^*$. The multiple scattering model calculation predicted that the double scattering contribution is significant at $-t \geqslant 0.4$ (GeV/c)^2, and the A_{yy} behaviour is defined by the spin structure of the deuteron and by the elementary amplitudes of the $NN \to NN^*$ and $NN^* \to NN^*$ processes.

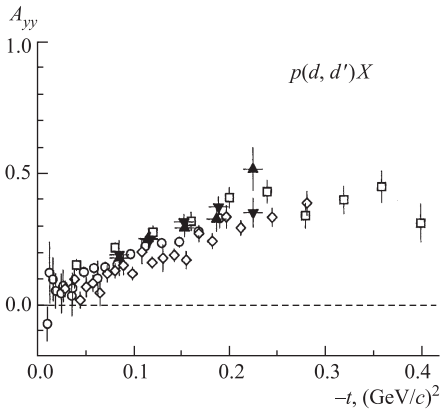

Fig. 30. Comparison of the tensor analyzing power data with the exclusive results. Black symbols — [183]: ▲ — $p(d,d')N\pi$; ▼ — $p(d,d')N\pi\pi$. Open symbols — this experiment: □ — 9 GeV/c; ○ — 5.5 GeV/c; ◇ — 4.5 GeV/c

The JINR inclusive inelastic A_y and A_{yy} data may be compared with the exclusive results obtained at Saturne II, using the SPES4-π setup [183]. The reactions:

- $d + p \to d + n + \pi^+$,
- $d + p \to d + p + \pi^0$, and
- $d + p \to d + N + \pi\pi$

have been measured at 3.73 GeV/c deuteron beam momentum. Figure 30 shows $A_{yy}(-t)$, and the authors conclude that the exclusive data values are systematically larger than the inclusive ones, which were obtained at nearby beam momentum.

The pion asymmetry was measured in the inclusive $d + A \to \pi^{\pm} + X$ processes at incident beam momenta from 3 to 9 GeV/c [165–167]. Pion emission angles were close to 90° in the laboratory frame. The vector analyzing power was determined using proton and carbon targets. Large vector analyzing power values and the π^+ and π^- asymmetries of opposite signs were observed with the hydrogen target at deuteron beam momenta from 3.5 to 6.5 GeV/c and at relatively low pion momenta in the range 300–350 MeV/c. The absolute value of A_y decreases with increasing beam and pion momenta. Evidence for nonzero values of the vector analyzing power was obtained with the carbon target. For this experiment the magnetic spectrometer DISK [165] was used.

Measurements of the asymmetry of pion, kaon and proton production by vector polarized deuterons on carbon nuclei were carried out at $T_{\rm kin}(d)$ 1.23 and

2.5 GeV/nucleon [168]. Secondary particles were detected at an angle $\theta_{\rm lab} = 24^\circ$. The magnetic channel of installation «KASPII» was used as the spectrometer. The particle momenta were 0.8 and 1.0 GeV. The authors observed a decrease of the asymmetry with increasing $T_{\rm kin}(d)$ and with increasing momenta of secondary particles.

6. PROTON–NUCLEUS ANALYZING POWER

The analyzing power in pC scattering, when only one charged particle is observed in a large detector, was determined. This experiment represents a special case of polarimetry. The results are often used for the second scattering, in which the polarization of particles, outgoing from an arbitrary reaction, is measured. Similar measurements were performed at TRIUMF, PSI, LAMPF, and Saturne II. The Dubna experiment (the responsible person was L. I. Sarycheva) uses polarized protons produced in the polarized deuteron break-up reaction on Be target. An accepted angular region is usually $3 \leqslant \theta_{\rm lab} \leqslant 25^\circ$, where the analyzing power is large enough and the differential cross-section value is not negligible. The results extended the available data region to high energy [184].

A_y was determined in an inclusive experiment at the SPHERE setup [185]. The vector analyzing power for quasi-elastic and inelastic scattering of polarized protons and deuterons on the C and CH_2 targets was measured. The energy of incident polarized deuterons was 3.6 GeV, that of polarized protons was either the same, or 2.51 GeV. The polarized proton beam was obtained as described in Subsec. 2.1.

LEADING PARTICLES Project. The investigation of interaction of polarized protons with nuclei is the subject of the new project «LEADING PARTICLES» at the Nuclotron. Authors propose measurements of single-spin asymmetries on intranuclear nucleons which can be compared with the analogous characteristics for the scattering on free nucleons in the energy region from 1.0 to 4.0 GeV. The first step will be the measurement of the analyzing power in pC scattering with the magnetic analysis of the scattered particle momentum, but without any separation of the quasi-elastic pp or pn interactions. The responsible person is L. I. Sarycheva.

SPIN Project. In the project «SPIN», it is planned to measure spin effects in NN and nucleon–nucleus interaction (and in nuclear decays) and to obtain the main spin observables in the reaction $np \to pp\pi^-$. The responsible person is M. Finger.

STRELA Project. In the experiment STRELA it is proposed to study a spin-dependent part of the nucleon scattering amplitude in the $np \to np$ scattering at $\theta_{\rm cm} = \pi$. Extracted polarized deuteron beam from the Nuclotron will be used. It is planned to measure the production cross section of two protons at small

momentum transfer in dp interactions in the region of deuteron momenta from 3.0 to 4.0 GeV/c. The spokespersons of this experiment are V. V. Glagolev and N. M. Piskunov.

ALPOM Experiment. New results of the analyzing power for the reacion p+CH_2 $\rightarrow$ one charged particle $+X$, at proton momenta of 1.75, 3.8, 4.5, and 5.3 GeV/c, were obtained. They extend the existing database for proton polarimetry at intermediate energies. The ALPOM apparatus, mentioned in Sec. 1, was used. The results confirm the feasibility of large acceptance polarimeter at high proton momenta. Particular attention was devoted to the investigation of the optimal target thickness and of the useful angular range.

The polarized protons were produced by fragmentation of the vector polarized deuteron beam on a 8-cm thick Be target, installed 60 m upstream of ALPOM. Two dipoles separated the break-up protons at zero angle from the deuteron beam and other produced particles. The angular and momentum acceptances of the beam transport line are $\Delta\Omega \simeq 10^{-4}$ sr and $\Delta p_p/p_p \simeq 3\%$. The average number of protons incident on the polarimeter was $\simeq 1.10^4$ per beam spill. Incident protons were detected by two proportional chambers from ALPHA [25]. Three wire chambers from POMME [32] were used to detect the trajectory of the scattered charged particle after the scattering on the CH_2 analyzer. Each chamber has x and y planes. The trigger was given by coincidence signals from two scintillation counters.

The target material was polyethylene. The analyzing powers A_y at $p_p = 3.8$ GeV/c for four target thicknesses (37.5, 51.6, 65.7, and 79.8 g/cm^2) are shown in Fig. 31, *a* where they are plotted as a function of $p_t = p_p(\mathrm{inc}) \times \sin\ \theta_{\mathrm{lab}}$. The shape and the absolute value are very similar and no systematic difference appears

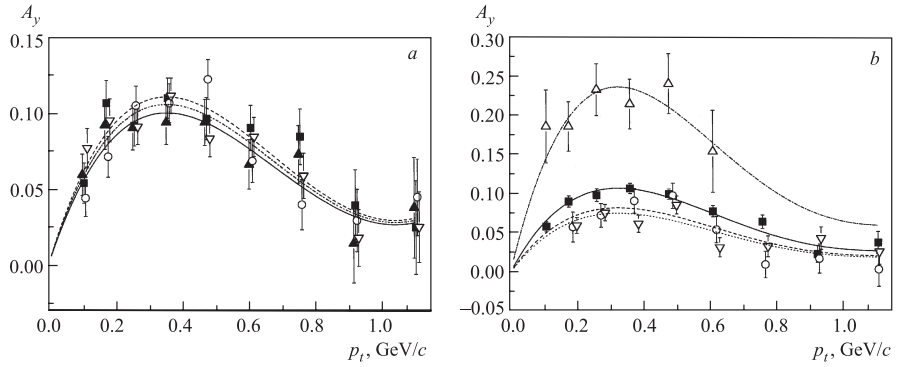

Fig. 31. Analyzing powers as a function of p_t (see text): *a*) for different CH_2 target thicknesses at $p_p = 3.8$ CeV/c: ▲ — 37.5 g/cm^2; ■ — 51.6 g/cm^2; ○ — 65.7 g/cm^2; ▽ — 79.8 g/cm^2; *b*) for different momenta with the CH_2 target of 51.6 g/cm^2: △ — 1.75 GeV/c; ■ — 3.8 GeV/c; ○ — 4.5 GeV/c; ▽ — 5.3 GeV/c

among the different sets of data. In Fig. 31, *b* are reported the data at each energy, summed over the target thickness. The curves are polynomial fits.

The spokespersons for the ALPOM experiments are C. F. Pedrisat, N. M. Piskunov and E. Tomasi-Gustafsson.

CONCLUSION

The Spin Physics has been a traditional experimental and theoretical field of fundamental research at JINR. Experiments started with the foundation of the Institute at the Synchrocyclotron of DLNP. The VBLHE staff extended the energy region of the spin-dependent experiments by the acceleration and extraction of polarized deuterons at the Synchrophasotron. The laboratory continued with the development of a high level accelerator — the Nuclotron, constructed with minimal funds. Due to common efforts, the attractive science at VBLHE survived the very difficult period following the decision to remove the Synchophasotron from the JINR budget. The instrumental and accelerator achievements obtained acknowledgements at foreign laboratories. Acceleration of polarized deuteron at the VBLHE accelerator complex, experimental equipment, polarimeters, targets, informatics and relevant physics are now attractive not only for the physicists from JINR Member States, but also for scientists from EU, USA, Japan, Canada, India, China, South Africa, and South America. This fact is confirmed by many fruitfull international cooperations. The large amount of scientific papers and contributions to international conferences in the field reflect a considerable number of original experiments in Dubna, providing new data recognized all over the world. The existence of the young new generation from different countries can be demonstrated by the number of theses on the relevant subjects.

Acknowledgements. The author wishes to thank E. B. Plekhanov, N. A. Piskunov, E. A. Strokovsky and E. Tomasi-Gustafsson for their kind help and assistance with the present review.

An abbreviated review on this subject was presented by the author at the JINR scientific council session and at the VBLHE scientific seminar in June 2001, as well as at the Varna conference in September 2001.

REFERENCES

1. *Rukoyatkin P. A.* // Czech J. Phys. B. 2004. V. 54. P. 179.
2. *Anisimov Yu. S. et al.* // Part. Nucl., Lett. 2004. V. 1, No. 1(118). P. 68.
3. *Anishchenko N. G. et al.* // J. Phys. (Paris). 1985. V. 46. P. C2–703.
4. *Ableev V. G. et al.* // Nucl. Instr. Meth. A. 1991. V. 306. P. 73.
5. *Avdeichikov V. V. et al.* JINR Preprint 13-84-20. Dubna, 1984.

6. *Avdeichikov V. V. et al.* JINR Preprint 10-90-106. Dubna, 1990.
7. *Cadmus R. R., Jr., Haeberli W.* // Nucl. Instr. Meth. 1975. V. 129. P. 403.
8. *Stephenson K., Haeberli W.* // Nucl. Instr. Meth. 1980. V. 169. P. 483.
9. *Abashidze L. I. et al.* // Prib. Tekh. Eksp. 1985. V. 4. P. 33.
10. *Avdeichikov V. V. et al.* // Yad. Fiz. 1989. V. 50. P. 409; Sov. J. Nucl. Phys. 1989. V. 50. P. 255.
11. *Alberi G., Bleszynski M., Jaroszewicz T.* // Ann. Phys. (N. Y.). 1982. V. 142. P. 299.
12. *Brody H. et al.* // Phys. Rev. C. 1981. V. 24. P. 2157.
13. *Artiomov A. S.* // JINR Rapid Commun. 1993. No. 4[61]. P. 6.
14. *Artiomov A. S.* // JINR Rapid Commun. 1994. No. 4[67]. P. 40.
15. *Artiomov A. S. et al.* // JINR Rapid Commun. 1996. No. 1[75]. P. 95.
16. *Baldin A. M. et al.* // JINR Rapid Commun. 1993. No. 4[61]. P. 13.
17. *Malakhov A. I. et al.* // Nucl. Instr. Meth. A. 2000. V. 440. P. 320.
18. *Ball J. et al.* // Eur. Phys. J. C. 1999. V. 11. P. 51.
19. *de Lesquen A. et al.* // Ibid. P. 69.
20. *Azhgirey L. S. et al.* // Part. Nucl., Lett. 2002. No. 4[113]. P. 51.
21. *Azhgirey L. S. et al.* // Prib. Tekh. Eksp. 1997. V. 1. P. 51; Instr. Exp. Tech. 1997. V. 40. P. 43.
22. *Glagolev V. V. et al.* JINR Preprint P1-88-6. Dubna, 1988.
23. *Glagolev V. V. et al.* // JINR Rapid Commun. 1995. No. 5[73]. P. 51.
24. *Issinsky I. B. et al.* // Acta Phys. Polon. B. 1994. V. 25. P. 673.
25. *Ableev V. G. et al.* // Prib. Tekh. Eksp. 1978. V. 3. P. 63.
26. *Ghazikhanian V. et al.* // Phys. Rev. C. 1991. V. 43. P. 1532.
27. *Arvieux J. et al.* // Phys. Rev. Lett. 1983. V. 50. P. 19.
28. *Arvieux J. et al.* // Nucl. Phys. A. 1984. V. 431. P. 613.
29. *Prokofiev A. N. et al.* Polarimeter for the deuteron beam at the JINR Synchrophasoton // Proc. of the 3rd Intern. Symp. «Dubna Deuteron-95», July 4–7, 1995. Dubna, 1996. P. 227–231.
30. *Azhgirey L. S. et al.* // JINR Rapid Commun. 1999. No. 3[95]. P. 20.
31. *Azhgirey L. S. et al.* // Nucl. Instr. Meth. A. 2003. V. 497. P. 340.
32. *Bonin B. et al.* // Nucl. Instr. Meth. A. 1991. V. 288. P. 379.
33. *Ladygin V. P.* // JINR Rapid Commun. 1999. No. 3[95]. P. 12.
34. *Afanasiev S. V. et al.* // Phys. Lett. B. 1998. V. 400. P. 1267.
35. *Afanasiev S. V. et al.* // Ibid. V. 434. P. 21.
36. *Azhgirey L. S. et al.* // Yad. Fiz. 1999. V. 62. P. 1796; Phys. At. Nucl. 1999. V. 62. P. 1673.
37. *Ladygin V. P. et al.* // Eur. Phys. J. A. 2000. V. 8. P. 409.
38. *Bystrický J., Lehar F., Winternitz P.* // J. Phys. (Paris). 1978. V. 39. P. 1.
39. *Froisart M., Stora M.* // Nucl. Instr. Meth. 1960. V. 7. P. 297.
40. *Plis Yu. A., Soroko F. N.* // Usp. Fiz. Nauk. 1973. V. 107. P. 281; Sov. Phys. Usp. 1973. V. 15. P. 318.
41. *Lechanoine-Leluc C., Lehar F.* // Rev. Mod. Phys. 1993. V. 65. P. 47.

42. *Bystrický J. et al.* // Nucl. Instr. Meth. A. 1985. V. 234. P. 412.
43. *Lehar F. et al.* // Nucl. Instr. Meth. A. 1995. V. 356. P. 673.
44. *Bazhanov N. A. et al.* // Nucl. Instr. Meth. A. 1996. V. 372. P. 349.
45. *Bazhanov N. A. et al.* // Nucl. Instr. Meth. A. 1998. V. 402. P. 484.
46. *Anishchenko N. G. et al.* // JINR Rapid Commun. 1998. No. 6[92]. P. 49.
47. *Bilenky S. M., Ryndin R. M.* // Phys. Lett. 1963. V. 6. P. 217.
48. *Phillips R. J. N.* // Nucl. Phys. 1963. V. 43. P. 413.
49. *Ball J. et al.* // Nuovo Cim. 1998. V. 111. P. 13.
50. *Bystrický J., Lechanoine-LeLuc C., Lehar F.* // Eur. Phys. J. C. 1998. V. 4. P. 607.
51. *Ball J. et al.* // Eur. Phys. J. C. 1998. V. 5. P. 57.
52. *Auer I. P. et al.* // Phys. Rev. Lett. 1981. V. 46. P. 1177.
53. *Lehar F. et al.* // Phys. Lett. B. 1987. V. 189. P. 241.
54. *Fontaine J.-M. et al.* // Nucl. Phys. B. 1991. V. 358. P. 297.
55. *Ball J. et al.* // Z. Phys. C. 1994. V. 61. P. 53.
56. *Binz R. et al.* // Nucl. Phys. A. 1991. V. 533. P. 601.
57. *Beddo M. et al.* // Phys. Lett. B. 1991. V. 258. P. 24.
58. *Haffter P. et al.* // Nucl. Phys. A. 1992. V. 548. P. 29.
59. *Brož J. et al.* // Z. Phys. A. 1997. V. 359. P. 23.
60. *Wilburn W. S. et al.* // Phys. Rev. C. 1995. V. 52. P. 2352.
61. *Brož J. et al.* // Z. Phys. A. 1996. V. 354. P. 401.
62. *Walston J. R.* Ph.D. Thesis. North Carolina State University, 1998.
63. *Raichle B. W.* Ph.D. Thesis. North Carolina State University, 1997.
64. *Ball J. et al.* // Proc. of the Intern. Workshop «Dubna Deuteron-91». Dubna, 1992. P. 12.
65. *Chernykh E. et al.* // Proc. of the Intern. Workshop «Dubna Deuteron-93». Dubna, 1994. P. 185; Proc. of the V Workshop on High Energy Spin Physics, Protvino, Sept. 20–24, 1993. Protvino, 1994. P. 478.
66. *Adiasevich V. P. et al.* // Z. Phys. C. 1996. V. 71. P. 65.
67. *Sharov V. I. et al.* // JINR Rapid Commun. 1996. No. 3[77]. P. 13.
68. *Sharov V. I. et al.* // JINR Rapid Commun. 1999. No. 4[96]. P. 17.
69. *Sharov V. I. et al.* // Eur. Phys. J. C. 2000. V. 13. P. 255.
70. *Sharov V. I. et al.* // Eur. Phys. J. C. 2004. V. 37. P. 79.
71. *Kirillov A. et al.* Relativistic Polarized Neutrons at the Laboratory of High Energy Physics, JINR. JINR Preprint E13-96-210. Dubna, 1996.
72. *Gorbunov N. V., Karev A. G.* // Proc. of the XII Intern. Symp. on Nuclear Electronics, Varna, Bulgaria, Sept. 12–18, 1988. Dubna, 1989. P. 103.
73. *Cheung E. et al.* // Phys. Lett. B. 1992. V. 284. P. 210.
74. *Nomofilov A. A. et al.* // Phys. Lett. B. 1994. V. 325. P. 327.
75. *Arndt R. A., Strakovsky I. I., Workman R. L.* // Phys. Rev. C. 2000. V. 62. P. 034005.
76. *Lee T.-S. H.* // Phys. Rev. C. 1984. V. 29. P. 195.

77. *Strakovsky I. I.* // Fiz. Elem. Chast. At. Yadra. 1991. V. 22. P. 615; Sov. J. Part. Nucl. 1991. V. 22. P. 296.

78. *Kopeliovich B. Z., Niedermayer F.* // Zh. Eksp. Teor. Fiz. 1984. V. 87. P. 1121; Sov. Phys. JETP. 1984. V. 60, No. 4. P. 640.

79. *Kopeliovich B. Z.* // Fiz. Elem. Chast. At. Yadra. 1990. V. 21. P. 117; Sov. J. Part. Nucl. 1990. V. 21, No. 1. P. 49.

80. *LaFrance P., Lomon E. L.* // Phys. Rev. D. 1986. V. 34. P. 1341.

81. *Gonzales P., LaFrance P., Lomon E. L.* // Phys. Rev. D. 1987. V. 35. P. 2142.

82. *LaFrance P.* // Can. J. Phys. 1990. V. 68. P. 1194.

83. *Lomon E. L.* // Colloque de Physique (France). 1990. V. 51. P. C6–363.

84. *LaFrance P., Lomon E. L.* // Proc. of the Intern. Conf. «Mesons and Nuclei at Intermediate Energies», Dubna, May 3–7, 1994. Singapore, 1995. V. XV. P. 97.

85. *Strokovsky E. A.* // Part. Nucl., Lett. 2004. V. 1, No. 2(119). P. 5.

86. *Lee T.-S., Riska D.* // Phys. Rev. Lett. 1993. V. 70. P. 2237.

87. *Bergdolt A. M. et al.* // Phys. Rev. D. 1993. V. 48. P. R2969.

88. *Chiavassa E. et al.* // Phys. Lett. B. 1996. V. 366. P. 39.

89. *Berger J. et al.* // Phys. Rev. Lett. 1988. V. 61. P. 61.

90. *Ellis J. et al.* // Phys. Lett. B. 1995. V. 353. P. 319.

91. *Ellis J., Gabathuler E., Karliner M.* // Phys. Lett. B. 1989. V. 217. P. 173.

92. *Alexakhin V. Yu. et al.* // JINR Rapid Commun. 1997. No. 2[82]. P. 81.

93. *Rekalo M. P., Arvieux J., Tomasi-Gustafsson E.* // Phys. Rev. C. 1997. V. 55. P. 2630.

94. *Ball J. et al.* // CTU Rep. (Prague). 2000. V. 4. P. 1.

95. *Allgower C. E. et al.* // Phys. Rev. C. 2001. V. 64. P. 034003.

96. *Arndt R. A. et al.* // Phys. Rev. C. 1997. V. 56. P. 3005.

97. *Kobushkin A. P.* // Phys. Lett. B. 1998. V. 421. P. 53.

98. *Kobushkin A. P.* // Yad. Fiz. 1999. V. 62. P. 1213; Phys. At. Nucl. 1999. V. 62. P. 1140.

99. *Frankfurt L. L., Strikman M. I.* // Phys. Rep. C. 1981. V. 76. P. 215.

100. *Strikman M. I., Frankfurt L. L.* // Yad. Fiz. 1978. V. 27. P. 1361; Sov. J. Nucl. Phys. 1978. V. 27. P. 717.

101. *Ableev V. G. et al.* // Nucl. Phys. A. 1983. V. 393. P. 491; 1984. V. 411. P. 591E.

102. *Ableev V. G. et al.* // JINR Rapid Commun. 1992. No. 1[54]. P. 10.

103. *Dolidze M. G., Lykasov G. I.* // Z. Phys. A. 1990. V. 336. P. 339.

104. *Lykasov G. I.* // Part. Nucl. 1993. V. 24. P. 140.

105. *Ableev V. G. et al.* // JETP Lett. 1983. V. 37. P. 196.

106. *Zaporozhets S. A. et al.* // Proc. of the VIII Intern. Seminar on High Energy Physics Problems, Dubna, June 1986. Dubna, 1987. P. 341.

107. *Blomquist K. I. et al.* // Phys. Lett. B. 1998. V. 424. P. 33.

108. *Azhgirey L. S. et al.* // Phys. Lett. B. 1996. V. 387. P. 37.

109. *Azhgirey L. S. et al.* // JINR Rapid Commun. 1996. No. 3[77]. P. 23.

110. *Aono T. et al.* // Phys. Rev. Lett. 1995. V. 74. P. 4997.

111. *Ableev V. G. et al.* // Pisma ZhETF. 1988. V. 47. P. 649; JETP Lett. 1988. V. 47. P. 558.
112. *Pedrisat C. F. et al.* // Phys. Rev. Lett. 1987. V. 59. P. 2840.
113. *Punjabi V. et al.* // Phys. Rev. C. 1989. V. 39. P. 608.
114. *Ableev V. G. et al.* // JINR Rapid Commun. 1996. No. 3[77]. P. 23.
115. *Dzikowski T. et al.* // JINR, E2-92-25. Dubna, 1992. P. 181.
116. *Kühn B. et al.* // Phys. Lett. B. 1994. V. 334. P. 298.
117. *Ableev V. G. et al.* // JINR Rapid Commun. 1990. No. 4[43]. P. 5.
118. *Borzunov Yu. T. et al.* // JINR Rapid Commun. 1997. No. 1[81]. P. 75.
119. *Afanasiev S. V. et al.* // JINR Rapid Commun. 1997. No. 4[84]. P. 5.
120. *Braun M. A., Tokarev M. V.* // Part. Nucl. 1991. V. 22. P. 1237.
121. *Glozman L. Ya. et al.* // Phys. Lett. B. 1988. V. 200. P. 983; Phys. Rev. C. 1993. V. 48. P. 389; Phys. Rev. C. 1994. V. 49. P. 1149; Phys. Lett. B. 1996. V. 381. P. 311.
122. *Kobushkin A. P.* // Proc. of the RCNP-TMU Symp. «Spins in Nuclear and Hadronic Reactions». Singapore, 2000. P. 223.
123. *Strokovsky E. A.* // JINR Rapid Commun. 1995. No. 2[70]. P. 29.
124. *Berthet P. et al.* // J. Phys. G: Nucl. Phys. 1982. V. 8. P. L111.
125. *Punjabi V. et al.* // Phys. Lett. B. 1995. V. 350. P. 178.
126. *Azhgirey L. S. et al.* // Phys. Lett. B. 1997. V. 391. P. 22.
127. *Azhgirey L. S. et al.* // Yad. Fiz. 1998. V. 61. P. 494; Phys. At. Nucl. 1998. V. 61. P. 432.
128. *Azhgirey L. S. et al.* // Czech J. Phys. 2004. V. 54. P. B243.
129. *Boivin M. et al.* // Few-Body Syst. 1999. V. 6. P. 1.
130. *Kühn B., Pedrisat C. F., Strokovsky E. A.* // Yad. Fiz. 1995. V. 58. P. 1898; Phys. At. Nucl. 1995. V. 58. P. 1794.
131. *Smirnov A. V., Uzikov Yu. N.* // Yad. Fiz. 1998. V. 61. P. 421; Phys. At. Nucl. 1998. V. 61. P. 336.
132. *Rekalo M. P., Piskunov N. M., Sitnik I. M.* // Few-Body Syst. 1998. V. 23. P. 187.
133. *Seyler R. G.* // Nucl. Phys. A. 1969. V. 124. P. 253.
134. *Rekalo M. P., Sitnik I. M.* // Phys. Lett. B. 1995. V. 356. P. 434.
135. *Sitnik I. M., Ladygin V. P., Rekalo M. P.* // Yad. Fiz. 1994. V. 57. P. 1270; Phys. At. Nucl. 1994. V. 57. P. 2089.
136. *Sitnik I. M., Ladygin V. P., Rekalo M. P.* // JINR Rapid Commun. 1994. No. 4[67]. P. 56.
137. *Sitnik I. M. et al.* // JINR Rapid Commun. 1995. No. 2[70]. P. 19.
138. *Kobushkin A. P. et al.* // Phys. Rev. C. 1994. V. 50. P. 2627.
139. *Afanasiev S. V. et al.* // Phys. Lett. B. 1998. V. 434. P. 21.
140. *Ladygin V. P. et al.* // Few-Body Syst. Suppl. 2000. V. 12. P. 240.
141. *Ladygin V. P. et al.* // Few-Body Syst. 2002. V. 32. P. 127.
142. *Analakyan K. V. et al.* // Yad. Fiz. 1977. V. 25. P. 545; Sov. J. Nucl. Phys. 1977. V. 25. P. 292.
143. *Stavinski K.V.* // Part. Nucl. 1979. V. 10, No. 6. P. 949.
144. *Nikoforov N. A. et al.* // Phys. Rev. C. 1980. V. 2. P. 700.
145. *Anderson L. et al.* // Phys. Rev. C. 1983. V. 28. P. 1224.

146. *Moeller E. et al.* // Ibid. P. 1246.
147. *Baldin A. M.* // Nucl. Phys. A. 1985. V. 434. P. 695.
148. *Kopeliovich V. B.* // Phys. Rep. 1986. V. 139. P. 52.
149. *Boyarinov S. V. et al.* // Yad. Fiz. 1989. V. 50. P. 1605; Sov. J. Nucl. Phys. 1989. V. 50. P. 996.
150. *Boyarinov S. V. et al.* // Yad. Fiz. 1991. V. 54. P. 119; Sov. J. Nucl. Phys. 1991. V. 54. P. 71.
151. *Gavrishchuck L. Ya. et al.* // Nucl. Phys. A. 1991. V. 523. P. 589.
152. *Belyaev I. M. et al.* // Yad. Fiz. 1993. V. 56. P. 135; Phys. At. Nucl. 1993. V. 56. P. 1378.
153. *Burov V. V., Lukyanov V. K., Titov A. I.* JINR Preprint P2-10244. Dubna, 1976.
154. *Lukyanov V. K., Titov A. I.* // Part. Nucl. 1979. V. 10, No. 4. P. 815.
155. *Baldin A. M.* JINR Preprint E2-83-415. Dubna, 1983.
156. *Efremov A. V. et al.* // Proc. of the XI Intern. Seminar on High Energy Physics Problems, Dubna, 1994. P. 309.
157. *Beznogikh G. G. et al.* // Yad. Fiz. 1991. V. 54. P. 1333; Sov. J. Nucl. Phys. 1991. V. 54. P. 812.
158. *Anisimov Yu. S. et al.* // JINR Rapid Commun. 1995. No. 5[73]. P. 31.
159. *Afanasiev S. V. et al.* // Nucl. Phys. A. 1997. V. 625. P. 817.
160. *Afanasiev S. V. et al.* // Phys. Lett. B. 1998. V. 445. P. 14.
161. *Schmidt I. A., Blankenbecler R.* // Phys. Rev. D. 1977. V. 15. P. 3321.
162. *Ch.-Y. Wong, Blankenbecler R.* // Phys. Rev. C. 1980. V. 22. P. 2433.
163. *Lacombe M. et al.* // Phys. Lett. B. 1981. V. 101. P. 139.
164. *Anisimov Yu. S. et al.* // Yad. Fiz. 1997. V. 60. P. 957; Phys. At. Nucl. 1997. V. 60. P. 1070.
165. *Averichev G. S. et al.* // JINR Rapid Commun. 1989. No. 4[37].
166. *Averichev G. S. et al.* // JINR Rapid Commun. 1995. No. 1[69]. P. 27.
167. *Averichev G. S. et al.* // Yad. Fiz. 1997. V. 60. P. 1799; Phys. At. Nucl. 1997. V. 60. P. 1643.
168. *Baldin A. A. et al.* // JINR Rapid Commun. 1995. No. 5[73]. P. 41.
169. *Banaigs J. et al.* // Phys. Lett. B. 1973. V. 45. P. 535.
170. *Baldini Celio R. et al.* // Nucl. Phys. A. 1982. V. 379. P. 477.
171. *Azhgirey L. S. et al.* // Yad. Fiz. 1978. V. 27. P. 1027; Sov. J. Nucl. Phys. 1978. V. 27. P. 544.
172. *Azhgirey L. S. et al.* // Yad. Fiz. 1979. V. 30. P. 1578; Sov. J. Nucl. Phys. 1979. V. 30. P. 818.
173. *Ableev V. G. et al.* // Yad. Fiz. 1983. V. 37. P. 348; Sov. J. Nucl. Phys. 1983. V. 37. P. 209.
174. *Azhgirey L. S. et al.* // Yad. Fiz. 1988. V. 48. P. 1758; Sov. J. Nucl. Phys. 1988. V. 48. P. 1058.
175. *Akimov Y. et al.* // Phys. Rev. Lett. 1975. V. 35. P. 763.
176. *Azhgirey L. S. et al.* // Phys. Lett. B. 1995. V. 361. P. 21.
177. *Azhgirey L. S. et al.* // JINR Rapid Commun. 1998. No. 2[88]. P. 17.
178. *Rekalo M. P., Tomasi-Gustafsson E.* // Phys. Rev. C. 1996. V. 54. P. 3125.
179. *Tomasi-Gustafsson E. et al.* // Phys. Rev. C. 1999. V. 59. P. 1256.
180. *Korovin P. P., Malinina L. V., Strokovsky E. A.* // JINR Rapid Commun. 1998. No. 6[92]. P. 35.
181. *Ladygin V. P. et al.* // Nucl. Phys. A. 2001. V. 8. P. 423c.
182. *Machleidt R., Holinde K., Elster K.* // Phys. Rep. 1987. V. 149. P. 1.
183. *Malinina L. V. et al.* // Phys. Rev. C. 2001. V. 64. P. 064001.
184. *Anoshina E. V. et al.* // Phys. At. Nucl. 1997. V. 60. P. 224.
185. *Yershov A. A. et al.* // Proc. of the XV Intern. Seminar on High Energy Physics Problems, Dubna, Sept. 25-29, 2000. Dubna, 2001. V.2. P. 54.
186. *Azhgirey L. S. et al.* JINR Preprint E1-2004-14. Dubna, 2004; Nucl. Instr. Meth. A (in press).